

MTL TR 89-10

AD

①

CRYSTAL CHEMISTRY, MAGNETIC AND ELECTRICAL PROPERTIES OF $La_{2-x}Ba_xNiO_4$

AD-A209 376

AMY B. AUSTIN
MATERIALS SCIENCE BRANCH

DTIC
ELECTE
MAY 23 1989
S D
Cb

February 1989

Approved for public release; distribution unlimited.



US ARMY
LABORATORY COMMAND
MATERIALS TECHNOLOGY LABORATORY

U.S. ARMY MATERIALS TECHNOLOGY LABORATORY
Watertown, Massachusetts 02172-0001

89 23 002

The findings in this report are not to be construed as an official Department of the Army position, unless so designated by other authorized documents.

Mention of any trade names or manufacturers in this report shall not be construed as advertising nor as an official indorsement or approval of such products or companies by the United States Government.

DISPOSITION INSTRUCTIONS

Destroy this report when it is no longer needed.
Do not return it to the originator.

UNCLASSIFIED

SECURITY CLASSIFICATION OF THIS PAGE (When Data Entered)

REPORT DOCUMENTATION PAGE		READ INSTRUCTIONS BEFORE COMPLETING FORM
1. REPORT NUMBER MTL TR 89-10	2. GOVT ACCESSION NO.	3. RECIPIENT'S CATALOG NUMBER
4. TITLE (and Subtitle) CRYSTAL CHEMISTRY, MAGNETIC AND ELECTRICAL PROPERTIES OF $\text{La}_{2-x}\text{Ba}_x\text{NiO}_4$		5. TYPE OF REPORT & PERIOD COVERED
		6. PERFORMING ORG. REPORT NUMBER
7. AUTHOR(s) Amy B. Austin		8. CONTRACT OR GRANT NUMBER(s)
9. PERFORMING ORGANIZATION NAME AND ADDRESS U.S. Army Materials Technology Laboratory Watertown, Massachusetts 02172-0001 SLCMT-EMS		10. PROGRAM ELEMENT, PROJECT, TASK AREA & WORK UNIT NUMBERS D/A Project: 1L161102AH42 ✓
11. CONTROLLING OFFICE NAME AND ADDRESS U.S. Army Laboratory Command 2800 Powder Mill Road Adelphi, Maryland 20783-1145		12. REPORT DATE February 1989
		13. NUMBER OF PAGES 78
14. MONITORING AGENCY NAME & ADDRESS (if different from Controlling Office)		15. SECURITY CLASS. (of this report) Unclassified
		15a. DECLASSIFICATION/DOWNGRADING SCHEDULE
16. DISTRIBUTION STATEMENT (of this Report) Approved for public release; distribution unlimited.		
17. DISTRIBUTION STATEMENT (of the abstract entered in Block 20, if different from Report)		
18. SUPPLEMENTARY NOTES Submitted to the Department of Materials Science and Engineering, MIT, in partial fulfillment of the requirements for the degree of Master of Science in Materials Science and Engineering.		
19. KEY WORDS (Continue on reverse side if necessary and identify by block number)		
K ₂ NiF ₄ structure	Lattice parameters	Electrical conductivity
Jahn-Teller effect	Chemical substitution	Oxide ceramics
Oxygen stoichiometry	Magnetic properties	Crystal chemistry
20. ABSTRACT (Continue on reverse side if necessary and identify by block number) (SEE REVERSE SIDE)		

UNCLASSIFIED

Block No. 20

ABSTRACT

The series of compositions $\text{La}_{2-x}\text{Ba}_x\text{NiO}_4$ ($0 \leq x \leq 1.0$) was prepared by standard ceramic techniques. All of the members of the system crystallized with the tetragonal K_2NiF_4 structure. The ratio of lattice parameters, c/a , reached a maximum in the range $x = 0.5$ to 0.6 ; c increased up to this point while a decreased, and this trend reversed after the maximum was reached. The increase in c/a is attributed to a weak Jahn-Teller distortion due to octahedral site low-spin Ni^{3+} ions. Magnetic susceptibilities measured in the temperature range 6 to 300 K and room temperature resistivity measurements showed that with the addition of any barium into the system, a significant change was seen in both the magnetic and electrical properties. An anomaly in the magnetic susceptibility was seen at 110 K in La_2NiO_4 . This anomaly disappeared and the magnetic susceptibility dropped by a factor of at least one-third with the addition of barium into the system. With further increases in barium, the susceptibility value did not differ significantly in all Ba-substituted compounds. The room temperature resistivity dropped from $0.14 \Omega\text{-cm}$ for La_2NiO_4 to $0.05 \Omega\text{-cm}$ for $\text{La}_{1.8}\text{Ba}_{0.2}\text{NiO}_4$ and decreased only slightly thereafter with increasing amounts of barium. Semiconducting behavior was observed for all of the compounds. Oxygen stoichiometry is suspected to play a critical role in the explanation of these behaviors.

Accession For	
NTIS CRASH	<input checked="" type="checkbox"/>
DTIC TAB	<input type="checkbox"/>
Unannounced	<input type="checkbox"/>
Justification	
By _____	
Distribution _____	
Additional Notes	
Dist	Availability or Special
A-1	

2
INS

CRYSTAL CHEMISTRY, MAGNETIC AND ELECTRICAL

PROPERTIES OF $\text{La}_{2-x}\text{Ba}_x\text{NiO}_4$

by

AMY BETH AUSTIN

S.B., Materials Science and Engineering
Massachusetts Institute of Technology
(1987)

Submitted to the Department of Materials Science and Engineering
in Partial Fulfillment of the Requirements
for the degree of Master of Science
in Materials Science and Engineering

at the

MASSACHUSETTS INSTITUTE OF TECHNOLOGY
February, 1989

© Amy B. Austin 1988

The author hereby grants to MIT permission to reproduce and to
distribute copies of this thesis document in whole or in part.

Signature of Author _____



Department of Materials Science & Engineering
Sept. 30, 1988

Certified by _____



James V. Marzik
Thesis Supervisor

Certified by _____

Yet-Ming Chiang
Associate Professor, Materials Science & Engineering
Thesis Supervisor

Accepted by _____

Samuel M. Allen
Chairman, Departmental Committee on Graduate Students

CRYSTAL CHEMISTRY, MAGNETIC AND ELECTRICAL PROPERTIES OF $\text{La}_{2-x}\text{Ba}_x\text{NiO}_4$

by
Amy Beth Austin

Submitted to the Department of Materials Science and Engineering
on January 20, 1989 in partial fulfillment of the requirements of the
degree of Master of Science in Materials Science and Engineering

Abstract

The series of compositions $\text{La}_{2-x}\text{Ba}_x\text{NiO}_4$ ($0 \leq x \leq 1.0$) was prepared by standard ceramic techniques. All of the members of the system crystallized with the tetragonal K_2NiF_4 structure. The ratio of lattice parameters, c/a , reached a maximum in the range $x = 0.5$ to 0.6 ; c increased up to this point while a decreased, and this trend reversed after the maximum was reached. The increase in c/a is attributed to a weak Jahn-Teller distortion due to octahedral site low-spin Ni^{3+} ions. Magnetic susceptibilities measured in the temperature range 6 to 300 K and room temperature resistivity measurements showed that with the addition of any barium into the system, a significant change was seen in both the magnetic and electrical properties. An anomaly in the magnetic susceptibility was seen at 110 K in La_2NiO_4 . This anomaly disappeared and the magnetic susceptibility dropped by a factor of at least one-third with the addition of barium into the system. With further increases in barium, the susceptibility value did not differ significantly in all Ba-substituted compounds. The room temperature resistivity dropped from $0.14 \Omega\text{-cm}$ for La_2NiO_4 to $0.05 \Omega\text{-cm}$ for $\text{La}_{1.8}\text{Ba}_{0.2}\text{NiO}_4$ and decreased only slightly thereafter with increasing amounts of barium. Semiconducting behavior was observed for all of the compounds. Oxygen stoichiometry is suspected to play a critical role in the explanation of these behaviors.

Company Supervisor: James V. Marzik
Title: Research Chemist, Army Materials Technology Laboratory

Thesis Supervisor: Yet-Ming Chiang
Title: Mitsui Associate Professor of Ceramics

Table of Contents

Title Page.....	1
Abstract.....	2
Table of Contents.....	3
Table of Illustrations and Figures.....	5
List of Tables.....	7
Acknowledgements.....	8
1. Introduction.....	9
1.1 Background.....	9
1.2 The K_2NiF_4 Structure.....	10
2. Experimental.....	12
2.1 Synthesis.....	12
2.2 X-ray Analysis.....	13
2.3 Microstructural Studies.....	13
2.4 Thermogravimetric Analysis.....	14
2.5 Magnetic Susceptibility Measurements.....	14
2.6 Electrical Resistivity Measurements.....	15
3. Results and Discussion.....	15
3.1 Crystal Structure.....	15
3.2 Microstructure.....	24
3.3 Oxygen Stoichiometry.....	24
3.4 Magnetic Properties.....	35
3.5 Electrical Properties.....	42
4. Conclusions and Directions for Future Research.....	45

Appendix A. Van der Pauw Technique.....	48
Appendix B. X-ray Diffraction Patterns for the Compositional Series La _{2-x} Ba _x NiO ₄ (0 ≤ x ≤ 1.0).....	52
Appendix C. Data From Cell Refinement Program.....	63
Appendix D. Magnetic Susceptibility Data - Curie-Weiss Law Plots.....	74
References.....	75

Table of Illustrations and Figures

1.1	K_2NiF_4 structure.....	11
3.1	Lattice parameters a and c versus Ba content for $La_{2-x}Ba_xNiO_4$	17
3.2	The ratio c/a versus Ba content for $La_{2-x}Ba_xNiO_4$	18
3.3	Cell volume versus Ba content for $La_{2-x}Ba_xNiO_4$	19
3.4	Microstructure of La_2NiO_4 and $La_{1.8}Ba_{0.2}NiO_4$	25
3.5	Microstructure of $La_{1.6}Ba_{0.4}NiO_4$ and $La_{1.4}Ba_{0.6}NiO_4$	26
3.6	Energy dispersive x-ray spectrum for La_2NiO_4	29
3.7	Energy dispersive x-ray spectrum for $La_{1.8}Ba_{0.2}NiO_4$	30
3.8	Energy dispersive x-ray spectrum for $La_{1.6}Ba_{0.4}NiO_4$	31
3.9	Energy dispersive x-ray spectrum for $La_{1.4}Ba_{0.6}NiO_4$	32
3.10	Magnetic susceptibility versus temperature for $La_{2-x}Ba_xNiO_4$ ($x = 0, 0.2, 0.4$ and 0.6).....	36
3.11	Magnetic Susceptibility of La_2NiO_4 measured by two methods.....	37
3.12	Room temperature electrical resistivity versus Ba content for $La_{2-x}Ba_xNiO_4$ ($x = 0, 0.2, 0.4$ and 0.6).....	43
A.1	Flat lamella of arbitrary shape.....	49
A.2	Flat lamella with line of symmetry.....	49
A.3	Graphical representation of van der Pauw's f factor.....	51
B.1	X-ray diffraction pattern for La_2NiO_4	52
B.2	X-ray diffraction pattern for $La_{1.9}Ba_{0.1}NiO_4$	53
B.3	X-ray diffraction pattern for $La_{1.8}Ba_{0.2}NiO_4$	54
B.4	X-ray diffraction pattern for $La_{1.7}Ba_{0.3}NiO_4$	55
B.5	X-ray diffraction pattern for $La_{1.6}Ba_{0.4}NiO_4$	56
B.6	X-ray diffraction pattern for $La_{1.5}Ba_{0.5}NiO_4$	57

B.7	X-ray diffraction pattern for $\text{La}_{1.4}\text{Ba}_{0.6}\text{NiO}_4$	58
B.8	X-ray diffraction pattern for $\text{La}_{1.3}\text{Ba}_{0.7}\text{NiO}_4$	59
B.9	X-ray diffraction pattern for $\text{La}_{1.2}\text{Ba}_{0.8}\text{NiO}_4$	60
B.10	X-ray diffraction pattern for $\text{La}_{1.1}\text{Ba}_{0.9}\text{NiO}_4$	61
B.11	X-ray diffraction pattern for LaBaNiO_4	62
D.1	Curie-Weiss law plots for $\text{La}_{2-x}\text{Ba}_x\text{NiO}_4$ ($x = 0, 0.2, 0.4$ and 0.6).....	74

List of Tables

3.1	Cell parameters for $\text{La}_{2-x}\text{Ba}_x\text{NiO}_4$ ($0 \leq x \leq 1$).....	16
3.2	Atomic percents of La, Ba and Ni present in $\text{La}_{2-x}\text{Ba}_x\text{NiO}_4$ ($0 \leq x \leq 0.6$).....	27
3.3	Magnetic constants for $\text{La}_{2-x}\text{Ba}_x\text{NiO}_4$ ($0 \leq x \leq 0.6$).....	40
C.1	Cell refinement data for La_2NiO_4	63
C.2	Cell refinement data for $\text{La}_{1.9}\text{Ba}_1\text{NiO}_4$	64
C.3	Cell refinement data for $\text{La}_{1.8}\text{Ba}_2\text{NiO}_4$	65
C.4	Cell refinement data for $\text{La}_{1.7}\text{Ba}_3\text{NiO}_4$	66
C.5	Cell refinement data for $\text{La}_{1.6}\text{Ba}_4\text{NiO}_4$	67
C.6	Cell refinement data for $\text{La}_{1.5}\text{Ba}_5\text{NiO}_4$	68
C.7	Cell refinement data for $\text{La}_{1.4}\text{Ba}_6\text{NiO}_4$	69
C.8	Cell refinement data for $\text{La}_{1.3}\text{Ba}_7\text{NiO}_4$	70
C.9	Cell refinement data for $\text{La}_{1.2}\text{Ba}_8\text{NiO}_4$	71
C.10	Cell refinement data for $\text{La}_{1.1}\text{Ba}_9\text{NiO}_4$	72
C.11	Cell refinement data for LaBaNiO_4	73

ACKNOWLEDGEMENTS

I would like to express my extreme gratitude to Dr. James Marzik and Dr. Louis Carreiro for the wisdom and patience they showed in guiding me throughout my stay at the Army Materials Technology Laboratory. I would also like to thank Dr. Marzik for the energy dispersive x-ray spectroscopy that he performed. I am also grateful to Dr. Paul Sagalyn, who kept me entertained with many an interesting story throughout the course of my research. I also would like to express my appreciation to Brown University for the use of their facilities and to Robert Kershaw for the Faraday balance measurement he performed for me at Brown University. In addition, I am thankful to Prof. Yet-Ming Chiang for his friendly support and patience when I chose to do things a little out of the ordinary. And, as always, I am grateful for the support and encouragement of my mother and father and Jill, Jeff and their families.

1. Introduction

1.1 Background

Although La_2NiO_4 was first reported in the late 1950's,¹ it was not until the 1970's that it began to attract attention. This first interest in La_2NiO_4 occurred when the significance of studying two-dimensional magnetic properties in oxides of the K_2NiF_4 structure was realized. Reports of two-dimensional antiferromagnetic ordering in K_2NiF_4 ² excited interest in studying the counterpart oxides (A_2BO_4) such as La_2NiO_4 , where the A ion is non-magnetic and the B ion is magnetic. The pursuit to establish the existence of long-range antiferromagnetic order in La_2NiO_4 has continued since that time. An anomaly in the magnetic susceptibility curve which showed up as a discontinuity in the Curie-Weiss law plots signaled the possible presence of antiferromagnetic order.^{3,4} Superlattice spots on electron diffraction patterns, similar to those observed for K_2NiF_4 , also indicated potential antiferromagnetic ordering;⁵ but neither neutron diffraction studies³ nor magnetic susceptibilities measured down to liquid helium temperature⁴ indicated the onset of any long-range ordering. The reason long-range order was not found in these early studies most likely is due to sample stoichiometry. La_2NiO_4 is very difficult to prepare stoichiometrically, with it usually being reported to have an oxygen excess.^{6,7,8} Both the magnetic and electrical properties of La_2NiO_4 have been shown to be very sensitive to the oxygen stoichiometry;^{6,7} thus, the lack of observed long-range order in these initial studies is likely due to the use of non-stoichiometric samples. Not until the mid-1980's, when experiments were conducted on stoichiometric single crystals, was long-range antiferromagnetic ordering found in La_2NiO_4 .⁶

The electrical properties of La_2NiO_4 have also made it of special interest. When it is oxygen-excess, it has a low electrical resistivity, with reported room temperature resistivities ranging from 0.03^7 to $0.3 \Omega\text{-cm}^5$. This, plus its high temperature stability (up to 1300°C in air), has made it of interest for applications such as electrodes in oxygen electrochemical gauges.⁹ It also exhibits a semiconductor-metal transition above 650 K ,⁶ which has been the focus of many studies.^{5,10,11}

Most recently, La_2NiO_4 has been studied because it possesses the same crystal structure as the new class of high temperature superconductors $\text{La}_{2-x}\text{M}_x\text{CuO}_4$ ($\text{M} = \text{Sr}$ or Ba) discovered by Bednorz and Müller.¹² The superconducting transition temperature for these compounds ranges from 30 to 45 K , which is higher than that predicted by the BCS theory of superconductivity.¹³ One possible path towards achieving a better understanding of the mechanism behind superconductivity in these materials lies in studying the properties of isostructural compounds, such as La_2NiO_4 . Structural and compositional studies of Sr- or Ba-substituted La_2NiO_4 (of the form $\text{La}_{2-x}\text{M}_x\text{NiO}_4$ ($\text{M} = \text{Sr}$ or Ba)) are also of interest, as formally there exists a mixed valence of Ni^{2+} and Ni^{3+} in these materials, which is similar in nature to the formal mixed valence state ($\text{Cu}^{2+}/\text{Cu}^{3+}$) present in the superconducting materials.

1.2 The K_2NiF_4 Structure

La_2NiO_4 possesses the K_2NiF_4 structure, which was originally described by Balz and Plieth¹⁴. The structure is made up of alternating rock-salt, AO, and perovskite, ABO_3 , layers, with the separation between layers being almost twice the intraplanar distance between two B ion nearest neighbors. (See Fig. 1.1.) This causes both the

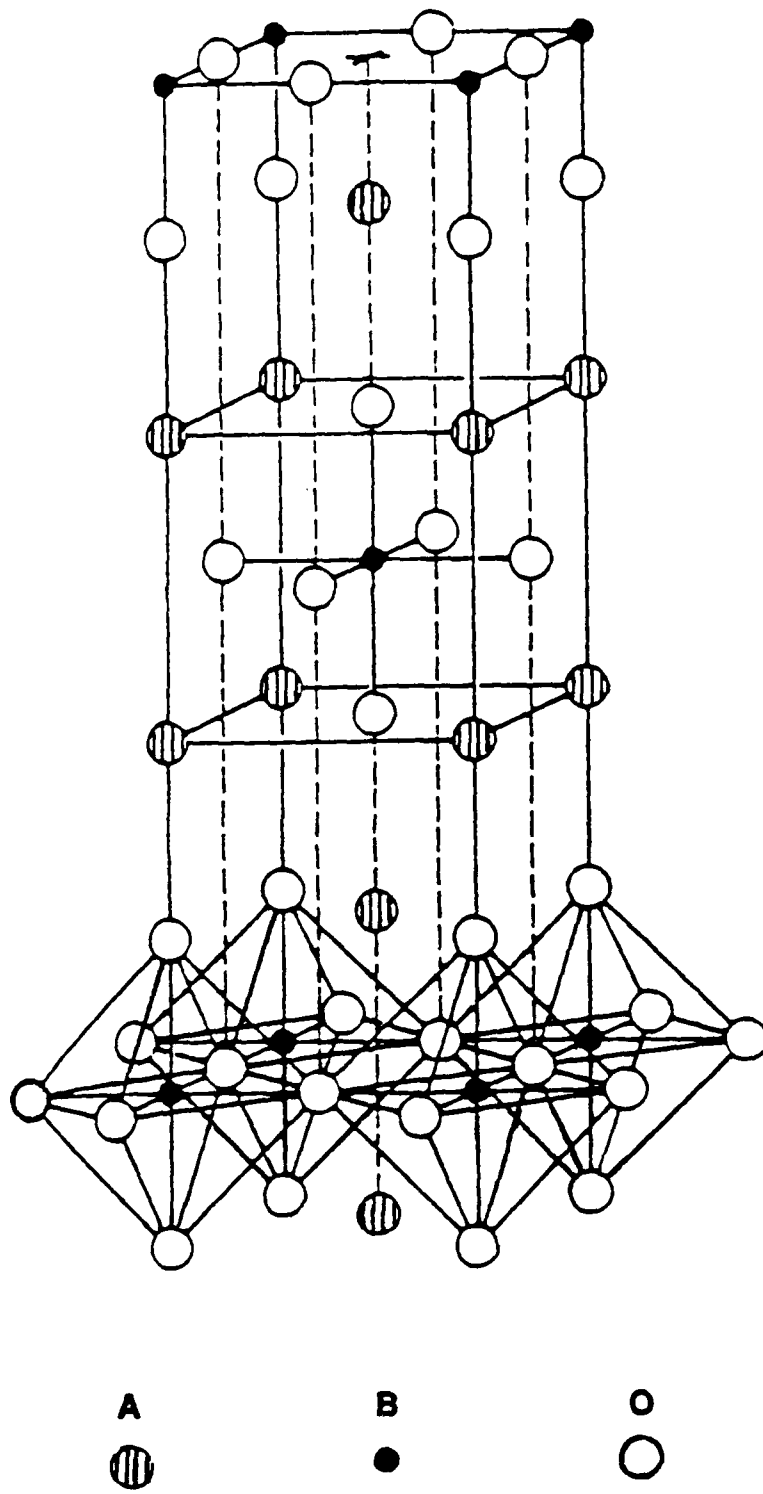


Figure 1.1 The K_2NiF_4 structure. For La_2NiO_4 the A atoms correspond to lanthanum, the B atoms to nickel and the O atoms to oxygen.

electrical and magnetic properties of materials possessing this crystal structure to be strongly two-dimensional. Of the many compounds which belong to this structure, most are halogenides or oxides. Various people¹⁵⁻¹⁷ have devised stability criteria for the oxides of this structure. One conceptually appealing model was proposed by Poix;¹⁷ it relates the stability of the structure to the ratio of the relative A - O - A and B - O - B bond lengths:

$$t = \frac{\sqrt{2} r(A - O)}{2 r(B - O)} \quad (2-1)$$

where the structure is stable for t within the limits $0.85 < t < 1.02$, and it is most stable for $t = 1.0$. The $\frac{\sqrt{2}}{2}$ factor arises because the {110} planes of the perovskite layers are stacked alternately with the {100} planes of the rock-salt layer.

2. Experimental

2.1 Synthesis

Solid solutions of the system $\text{La}_{2-x}\text{Ba}_x\text{NiO}_4$ ($0 \leq x \leq 1.0$) were prepared using the appropriate stoichiometric amounts of 99.99% La_2O_3 , NiO and BaCO_3 . The mixtures were thoroughly ground using an agate mortar and pestle, followed by dissolution in a minimum amount of nitric acid (HNO_3), which produced an emerald green paste.* The mixtures were heated overnight at 150°C , followed by another grinding and a 12-hour firing at 600°C to burn off the nitrates.** After this step the powders appeared dark gray in color. They were then reground and fired in

* This nitration technique was used as it was shown to provide more intimate mixing, more chemically homogeneous products and shorter reaction times compared with standard solid state reaction of the oxides.

** Alumina crucibles or plates were used for all firings.

air at 1100° C for 24 to 36 hours with 1 to 2 intermittent grindings, after which the powders were black in color.

Sintered pellets were made from the powder in order to measure the magnetic and electrical properties of the materials. Pellets were formed in a Carver® press and sintered at temperatures ranging from 1150° C to 1250° C for 12 hours in air. It was found that the sintering temperature decreased with increasing barium content.

2.2 X-ray Analysis

Powder diffraction patterns of the samples were obtained with a Philips-Norelco diffractometer using monochromated high intensity $\text{CuK}\alpha_1$ radiation ($\lambda = 1.5405\text{\AA}$). For qualitative identification of the phases present, the patterns were taken from $12^\circ \leq 2\theta \leq 72^\circ$ with a scan rate of $1^\circ 2\theta/\text{min}$ and a chart speed of 30 in/hr. The scan rate used to obtain more quantitative analyses was $0.25^\circ 2\theta/\text{min}$ with a chart speed of 30 in/hr. Cell parameters were then determined using a least squares refinement of the measured reflections.¹⁸

2.3 Microstructural Studies

The microstructure of sintered samples of $\text{La}_{2-x}\text{Ba}_x\text{NiO}_4$ ($x = 0, 0.2, 0.4$ and 0.6) was examined using a JEOL 840 scanning electron microscope (SEM). The atomic ratios of lanthanum, barium and nickel present in these samples were determined by energy dispersive x-ray spectroscopy (EDS) using a Tracor Northern 5500 x-ray and image analyzer. For each sample, spectra were gathered on five different points for 100 seconds each. Quantitative analyses were performed using a Tracor Northern least squares spectral fitting program.¹⁹ Data on all of spectra

were corrected for atomic number, absorption and fluorescence effects using a standard ZAF program. For these corrections, a single crystal of LaB_6 was used as the lanthanum standard, a BaSO_4 sample, commercially available from Tousimis, for the barium standard, and a nickel sample, also commercially available from Tousimis, for the nickel standard.

2.4 Thermogravimetric Analysis

Oxygen stoichiometries were determined on powder samples of the La_2NiO_4 and $\text{La}_{1.4}\text{Ba}_{0.6}\text{NiO}_4$ compounds by thermogravimetric analysis (TGA) using a Cahn electrobalance (Model RG). In these studies a reducing atmosphere of predried 85% Ar/15% H_2 was passed over the sample. Approximately 50 mg of compound was used for each experiment. The sample bucket was initially fired to 1000°C in order to burn off any possible contaminants that would affect the experiment and then allowed to cool to room temperature before adding the sample. After the room temperature weight had stabilized, the sample was heated to 1000°C at a rate of $1^\circ/\text{min}$ under a gas flow of $60\text{ cm}^3/\text{min}$. The reduction was allowed to continue until a constant weight was reached. An x-ray diffraction pattern was then taken of the reduced sample.

2.5 Magnetic Susceptibility Measurements

DC magnetic susceptibility measurements were done for the temperature range 6 to 300 K on sintered samples of $\text{La}_{2-x}\text{Ba}_x\text{NiO}_4$ ($x = 0, 0.2, 0.4$ and 0.6) using a S.H.E. Corp. SQUID magnetometer. Readings were taken for each temperature after the temperature had remained stable for five minutes to within $\pm 0.02\text{ K}$ for $T < 70\text{ K}$ and to within $\pm 0.1\text{ K}$ for $70 \leq T \leq 300\text{ K}$. The magnetic susceptibility was also measured for the temperature range 77 to 300 K on a powder sample of

La_2NiO_4 using a Faraday balance described elsewhere.²⁰ The balance was calibrated with platinum wire ($\chi_g = 0.991 \times 10^{-6}$ emu/g at 275 K). Corrections were applied to compensate for the effect of the quartz sample bucket. No corrections for core diamagnetism were made on any of the magnetic measurements.

2.6 Electrical Resistivity Measurements

Room temperature resistivity measurements were taken on sintered samples of $\text{La}_{2-x}\text{Ba}_x\text{NiO}_4$ ($x = 0, 0.2, 0.4$ and 0.6) using the van der Pauw four-point probe technique. (See Appendix A.) Indium leads were attached to the circumference of the samples using an ultrasonic soldering iron. This method enabled approximate point contacts to be made with the sample. In addition, the changing trend in resistivity was qualitatively noted as the sample was cooled down to 77 K.

3. Results and Discussion

3.1 Crystal Structure

X-ray analysis showed that members of the system $\text{La}_{2-x}\text{Ba}_x\text{NiO}_4$ ($0 \leq x \leq 1.0$) were single phase (Appendix B) and crystallize with the tetragonal K_2NiF_4 structure. Table 3.1 lists the cell dimensions for the compounds. Individual reflections from the cell refinements are given in Appendix C. With increasing barium ($0 \leq x \leq 0.5$), the cell elongates in the c -direction and compresses in the a - b plane, with the cell volume staying roughly constant. Within the compositional range ($0.5 \leq x \leq 0.6$), the trend reverses. The c parameter reaches a maximum and decreases slightly thereafter, while the a parameter reaches a minimum and,

Table 3.1 Tetragonal Cell Parameters for the Compositional Series
 $\text{La}_{2-x}\text{Ba}_x\text{NiO}_4$ ($0 \leq x \leq 1.0$):

Compound	a (Å)	c (Å)	V (Å ³)
La_2NiO_4	3.859(1)	12.679(1)	188.80(4)
$\text{La}_{1.9}\text{Ba}_{0.1}\text{NiO}_4$	3.858(1)	12.727(1)	189.47(3)
$\text{La}_{1.8}\text{Ba}_{0.2}\text{NiO}_4$	3.855(1)	12.764(1)	189.73(3)
$\text{La}_{1.7}\text{Ba}_{0.3}\text{NiO}_4$	3.848(1)	12.813(2)	189.70(5)
$\text{La}_{1.6}\text{Ba}_{0.4}\text{NiO}_4$	3.845(1)	12.843(2)	189.89(4)
$\text{La}_{1.5}\text{Ba}_{0.5}\text{NiO}_4$	3.842(1)	12.860(5)	189.83(8)
$\text{La}_{1.4}\text{Ba}_{0.6}\text{NiO}_4$	3.847(1)	12.888(3)	190.76(5)
$\text{La}_{1.3}\text{Ba}_{0.7}\text{NiO}_4$	3.853(1)	12.877(2)	191.12(4)
$\text{La}_{1.2}\text{Ba}_{0.8}\text{NiO}_4$	3.858(1)	12.858(3)	191.35(6)
$\text{La}_{1.1}\text{Ba}_{0.9}\text{NiO}_4$	3.865(1)	12.850(2)	191.97(4)
LaBaNiO_4	3.868(1)	12.839(3)	192.13(5)

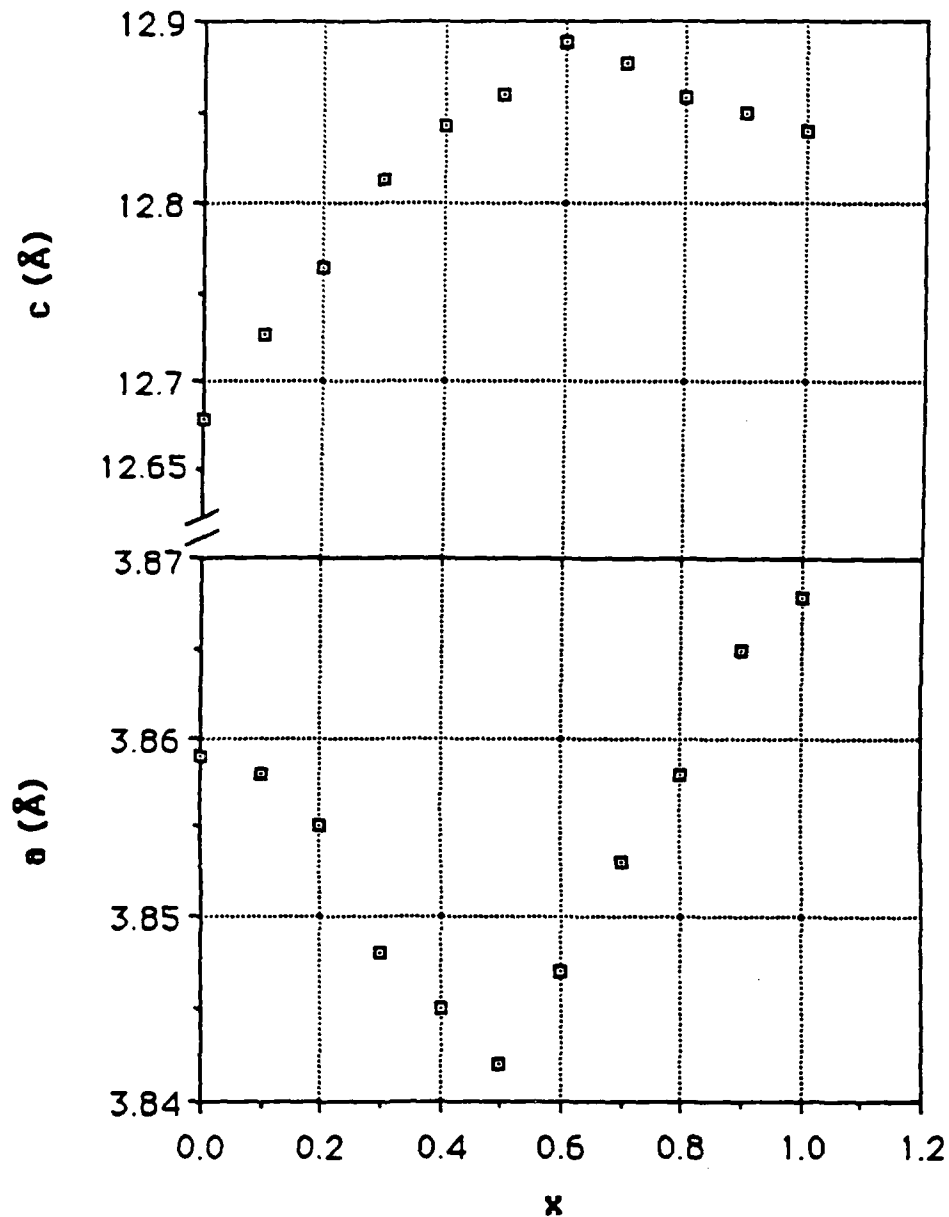


Figure 3.1. Change in the tetragonal cell parameters a and c with increasing Ba content in $\text{La}_{2-x}\text{Ba}_x\text{NiO}_4$. The initial increase in c and corresponding decrease in a is due to a Jahn-Teller distortion. The later increase in a is attributed to a steric effect caused by the increasing amount of Ba being substituted for the smaller La ion. The slight decrease in c in this region is explained as a result of lessening of electrostatic repulsion. The presence of Ni^{4+} in compounds with higher concentrations of barium ($x \geq 0.5$) could also help explain this behavior.

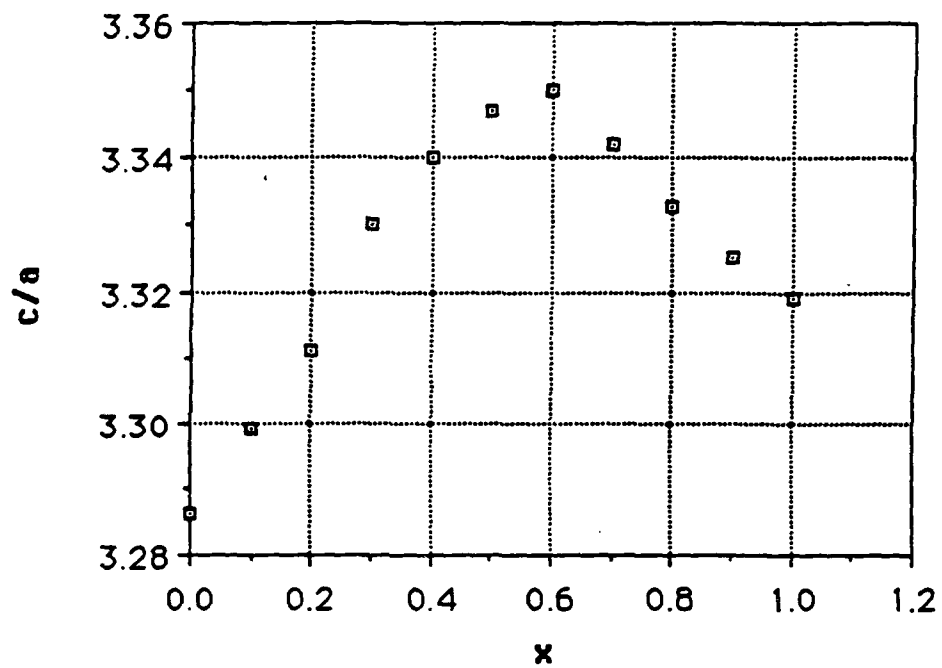


Figure 3.2. Change in the ratio of lattice parameters, c/a , with increasing Ba content in $\text{La}_{2-x}\text{Ba}_x\text{NiO}_4$. The overall effect of the Jahn-Teller distortion reaches a maximum at $x = 0.6$.

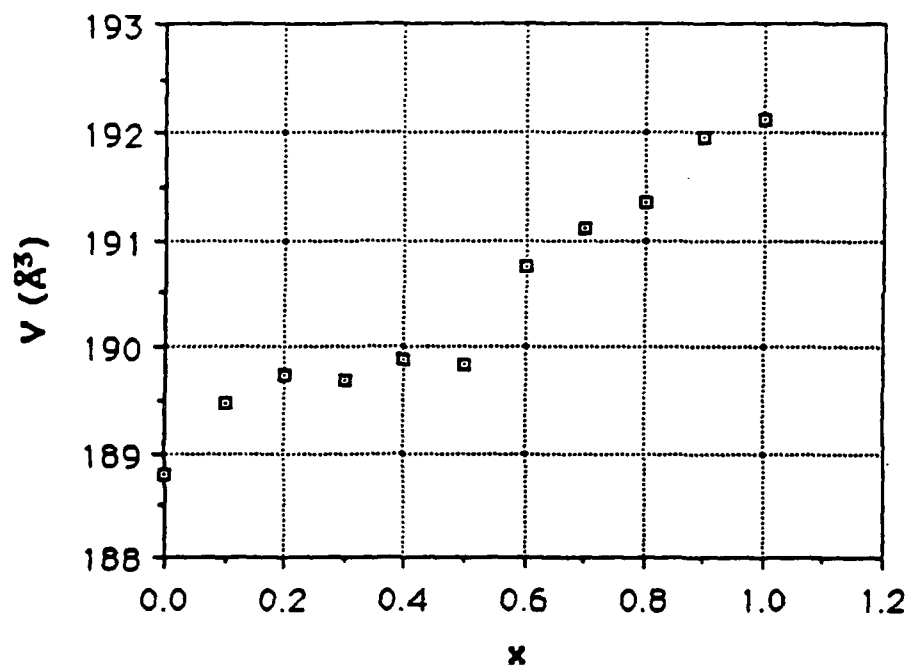


Figure 3.3. Change in cell volume with increasing Ba content in $\text{La}_{2-x}\text{Ba}_x\text{NiO}_4$. The volume stays roughly constant in the region where only the Jahn-Teller distortion is present. As steric effects also begin to affect the cell parameters, forcing the a - b plane to expand, the volume begins to increase.

then starts to increase sharply. At this point, the volume also starts to increase at a steady rate. (See Figs. 3.1 and 3.3.) Cell refinements were done on a second series of separately-prepared compounds, reproducing the results of this first study.

The initial increase in c and corresponding decrease in a with increase in barium content is understandable with respect to the change in the oxidation state of nickel. For stoichiometric La_2NiO_4 , formally, only Ni^{2+} should exist. As barium is substituted into $\text{La}_{2-x}\text{Ba}_x\text{NiO}_4$, an equal amount of Ni^{2+} is oxidized to Ni^{3+} in order to preserve electrical neutrality.* The trivalent nickel created by barium substitution may exist in either the low-spin ($t_{2g}^6e_g^1$) or high-spin ($t_{2g}^5e_g^2$) state. For the similar compositional series, $\text{La}_{2-x}\text{Sr}_x\text{NiO}_4$,²¹ (as well as many other trivalent nickel-oxide systems, such as LaNiO_3 and NaNiO_2)^{23,24}, it is reported to exist in the low-spin state.

Gopalakishnan *et al.*²¹ reason that since the Ni - O - Ni distance in the $\text{La}_{2-x}\text{Sr}_x\text{NiO}_4$ system ($< 3.87 \text{ \AA}$) is smaller than that for NiO (4.177 \AA), the trivalent nickel exists in the low-spin state. This low-spin state, $t_{2g}^6e_g^1$, is susceptible to Jahn-Teller distortions which could shorten the Ni - O - Ni bond length. In the present system the Ni - O - Ni distance ($< 3.87 \text{ \AA}$) is also smaller than that for NiO, so it is reasonable to expect that here, too, the trivalent nickel exists in the low-spin state. In this state there exist octahedrally-coordinated, d^7 ions which are orbitally degenerate because the "hole" in the d^6 configuration may be either the d_{z^2} or the $d_{x^2-y^2}$ orbital of the e_g -set. The fact that the c -axis elongates while the a - b plane compresses (for $0 \leq x \leq 0.5-0.6$) appears to indicate that the distortion of the low-spin state Ni^{3+} -O octahedra is to produce four short and two long bonds and, therefore, that the single e_g electron is ordered in the d_{z^2} orbital.

* This series can therefore be formulated as $\text{La}_{2-x}^{3+}\text{Ba}_x^{2+}\text{Ni}_{1-x}^{2+}\text{Ni}_x^{3+}\text{O}_4^{2-}$.

The Jahn-Teller distortion reaches a maximum at $x = 0.6$ (Fig. 3.2), where the c/a ratio equals 3.350. For the tetragonal K_2NiF_4 structure, the c/a ratio normally lies between 3.25 and 3.30, except when a Jahn-Teller ion is present.^{8,24} For instance, Jahn-Teller distortions are evident for K_2CuF_4 which has a c/a ratio of 3.07, La_2CuO_4 having a c/a ratio of 3.46²⁵ and $La_2Ni_{0.5}Li_{0.5}O_4$, a Ni^{3+} -containing compound, with a c/a ratio of 3.43.²⁶ As 3.350, the maximum c/a ratio seen in $La_{2-x}Ba_xNiO_4$, varies only slightly from the normal c/a value, the Jahn-Teller distortion appears to be relatively weak for this system. This was also found to be the case for $La_{2-x}Sr_xNiO_4$.²¹

The decrease in the a -axis in the region $0 \leq x \leq 0.5$ is further enhanced by the fact that the ionic radius of Ni^{3+} in the low-spin state (0.56 Å) is much smaller than that of Ni^{2+} (0.69 Å). This takes place even though the A-ion size is concurrently being increased as a result of Ba^{2+} substitution for La^{3+} .^{*} This is easily understood with respect to the K_2NiF_4 structure. The alternating perovskite and rock-salt layers give the structure rigidity. From a purely ionic view,²⁷ for La_2NiO_4 , the B - O - B^{**} bond length should equal 4.18 Å, while the corresponding bond length $\frac{\sqrt{2}}{2}(A - O - A)^\dagger$ in the rock-salt structure should be 3.68 Å. This difference causes buckling of the BO_6 octahedra in $LaNiO_3$ ⁸, but the intervening rock-salt layer (present in the K_2NiF_4 structure) does not allow that to happen for La_2NiO_4 . Instead, the perovskite layer is put in compression, while the rock-salt layer is put into tension. Thus, the measured a parameter, 3.859 Å, is

* The volume also stays constant in this range, even though increasing amounts of a larger ion are being substituted into the compound. This is in contradiction to Vegard's rule.

** The B ions correspond to either Ni^{2+} or Ni^{3+} , while the A ions correspond to either La^{3+} or Ba^{2+} .

† The {110} planes of the perovskite layers are stacked alternately with the {100} planes of the rock-salt layer.

less than what would be expected by only considering the B - O - B bond length and more than that which would be expected by considering just the rock-salt layer. The Jahn-Teller distortion, however, causes a to be significantly less than the average of these two. As barium is substituted onto the A-site, the A - O - A bond lengthens because of the larger barium ion and the B - O - B bond shortens because of the oxidation of nickel. The calculated B - O - B distance, therefore, continues to decrease down to a value of 3.92 Å, while the A - O - A distance increases up to a value of 3.87 Å for LaBaNiO₄; thus, in the compositional range studied, taking into account only ionic effects, the larger size of the barium ion should never force the a -axis to expand and, in fact, the oxidation of the nickel due to the barium substitution allows it to initially decrease.

The fact that the a parameter does increase (after a minimum value is reached) is a combined result due to the presence of the Jahn-Teller ion and the replacement of lanthanum by the larger barium ion. The Jahn-Teller ion creates a configuration in which the energy is lowered by a shortening of the bonds in the a - b plane. This decrease in a puts the B - O - B bond in even greater compression, but, at least initially, also serves to lessen the tension on the A - O - A bond. The a parameter reaches a minimum value of 3.842 Å for La_{1.5}Ba_{0.5}NiO₄, at which point the calculated value for the B - O - B bond is 4.05 Å, while the corresponding bond length, $\frac{\sqrt{2}}{2}(A - O - A)$, is 3.77 Å. At this point, then, the tension on the A - O - A bond is still being slightly lessened by the Jahn-Teller distortion in the a - b plane. But as the barium concentration increases further, this situation changes; the A - O - A distance continues to increase and the B - O - B length to decrease, with the average of the two staying close to 3.90 Å. As further decreases in a no longer serve to lessen the tension in the rock-salt layer, the structure becomes less susceptible to the Jahn-Teller distortion, and the pure size of the ions forces a to

start to increase, easing some of the compression now present in both structural layers. Weak Jahn-Teller distortions continue to play a role, however, as the measured a value for LaBaNiO_4 is less than that calculated for either the rock-salt or perovskite layer. There may also be covalent effects present which could cause the lattice parameters to vary slightly from that which has been discussed here.

Although weak Jahn-Teller distortions are still present, the c -axis slightly decreases in the same region where the a -axis is increasing.* This is attributed to a lessening of electrostatic repulsion. Along the c -axis there are A-O-B-O-A...A-O-B-O-A linkages. (See Fig. 1.1.) Thus, strong electrostatic repulsion exists between A...A ions, which have no anions intervening between them. As the La^{3+} ions are replaced by Ba^{2+} ions, this electrostatic repulsion lessens, allowing the c -axis to pack together a little more tightly. Ganguly and Rao⁸ propose that this electrostatic repulsion is also a factor in making the a parameter less than what is expected from ionic radii. They believe that oxygen ions in the basal plane may actually draw closer together in order to help screen the electrostatic repulsion between the A...A ions. This model is in complete agreement with what is seen in the present system. With higher concentrations of barium (where the electrostatic repulsion is undoubtedly lessened), the c -axis contracts slightly as the A...A ions feel less repulsion towards one another and the a -axis expands, as the oxygen ions no longer have as large of an electrostatic repulsion to shield.

Gopalakishnan *et al.*²¹ explain similar behavior observed in the $\text{La}_{2-x}\text{Sr}_x\text{NiO}_4$ system by saying that the low-spin state changes so that the e_g electron becomes ordered in the $d_{x^2-y^2}$ orbital. In the present system, however, even though overall a is increasing, the a parameter continues to be less than the

* This is possible because the a - b plane is the plane of densest packing.

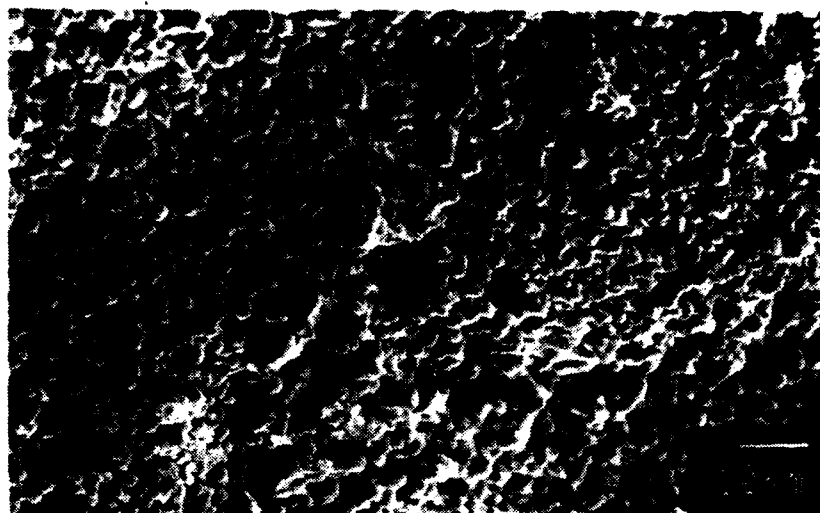
average value of the B - O - B and corresponding A - O - A bond lengths, indicating that the eg electron is still aligned along the d_{z^2} orbital.

Preliminary studies indicate another possible factor. TGA performed on $\text{La}_{1.4}\text{Ba}_{0.6}\text{NiO}_4$ seems to indicate a three-step reduction, which may correspond to the presence of Ni^{2+} , Ni^{3+} and Ni^{4+} in the Ba-substituted compound.* It has been suggested²⁸ that alkaline earth ions can stabilize Ni^{4+} in the system $\text{La}_{1-x}\text{M}_x\text{NiO}_3$ (M = Ca, Ba or Sr). The ionic radius of Ni^{4+} is slightly less than that of Ni^{3+} , but the Ni^{4+} , d^6 electronic configuration is not susceptible to a Jahn-Teller distortion; thus the presence of Ni^{4+} for the range of barium concentrations $0.6 \leq x \leq 1.0$ would be consistent with the lattice parameter data in this work. The Jahn-Teller distortion due to the Ni^{3+} , d^7 ions would be reduced in these high Ba-containing compounds, and their lattice parameters would actually correspond closely to those of compounds with lower barium concentrations, but with equal Ni^{3+} concentrations.

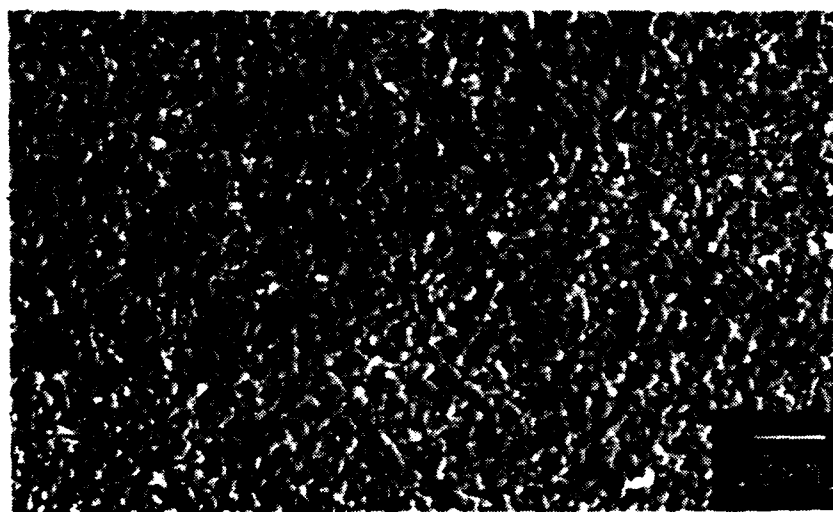
3.2 Microstructure

SEM showed the particle size to be under 10 microns in all of the measured samples. In addition, it showed that the particle size was especially uniform for all Ba-substituted samples. (See Figs. 3.4 and 3.5.) The particle size is also smaller in the Ba-substituted samples, as would be expected due to their lower sintering temperature.

* For La_2NiO_4 only a two-step reduction is apparent, which would correspond to only Ni^{2+} and Ni^{3+} .



a) La_2NiO_4

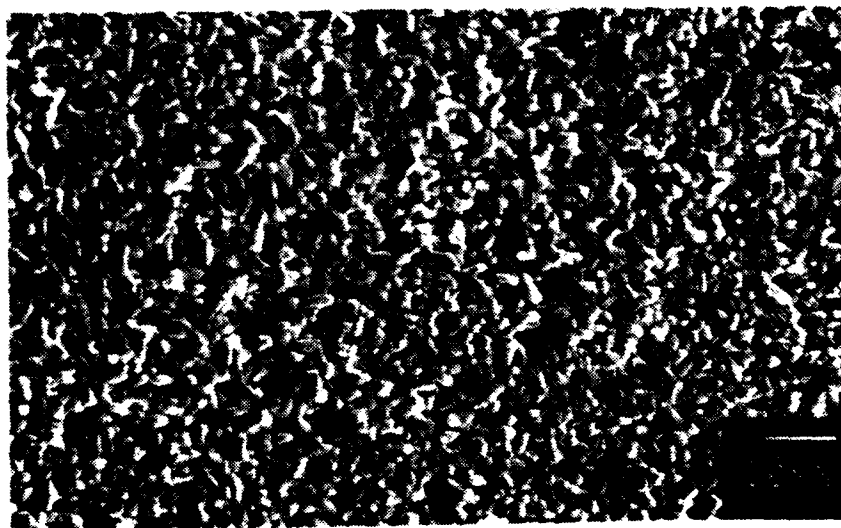


b) $\text{La}_{1.8}\text{Ba}_{0.2}\text{NiO}_4$

Figure 3.4 Microstructure of a) La_2NiO_4 and b) $\text{La}_{1.8}\text{Ba}_{0.2}\text{NiO}_4$.



a) $\text{La}_{1.6}\text{Ba}_{0.4}\text{NiO}_4$



b) $\text{La}_{1.4}\text{Ba}_{0.6}\text{NiO}_4$

Figure 3.5. Microstructure of a) $\text{La}_{1.6}\text{Ba}_{0.4}\text{NiO}_4$ and b) $\text{La}_{1.4}\text{Ba}_{0.6}\text{NiO}_4$.

The relative atomic percents of lanthanum, barium and nickel present in the samples were measured by EDS. The results from this technique are given in Table 3.2 and plotted spectra for each sample are shown in Figs. 3.6 - 3.9. The calculated values correspond to the expected values (for the given sample stoichiometry) to within the error of the measurement and technique. In addition, the consistency in values measured from different points on the sample indicates that the materials microchemically homogeneous. Sayer and Odier⁷ saw a slight lanthanum deficiency ($\text{La/Ni} = 1.985 - 1.99$) in La_2NiO_4 prepared by reaction of the oxides. This differs from the present work in that nitrate precursors were not used. Furthermore, much higher temperatures and longer heating times were used as compared to those employed in the present work. The material was reacted at 1200°C and sintered at 1300°C for 48 hours, as opposed to the present study where the materials were reacted at 1100°C and sintered at $1150 - 1250^\circ\text{C}$ for 12 hours.

3.3 Oxygen Stoichiometry

The oxygen stoichiometries were determined on La_2NiO_4 and $\text{La}_{1.4}\text{Ba}_{0.6}\text{NiO}_4$ compounds by TGA. X-ray diffraction patterns of the reduced compounds showed La_2O_3 and nickel metal, and also BaO for the Ba-containing compound. The measured weight losses, with respect to these reductions, indicated an excess of oxygen for both samples.* This corresponded to an actual stoichiometry of $\text{La}_2\text{NiO}_{4.13}$ for the La_2NiO_4 sample and $\text{La}_{1.4}\text{Ba}_{0.6}\text{NiO}_{4.08}$ for the Ba-substituted sample.**

* This was also taking into account that the cation atomic ratios had been determined to be as expected.

** Up to this point, these compounds have been referred to as La_2NiO_4 and $\text{La}_{1.4}\text{Ba}_{0.6}\text{NiO}_4$ -- and may continue to be referred to as such -- out of simplicity. In addition, most likely the other compounds are also oxygen-rich, but measurements to determine this have as yet not been made.

Table 3.1 Relative atomic percents of La, Ba and Ni measured for the samples $\text{La}_{2-x}\text{Ba}_x\text{NiO}_4$ ($x = 0, 0.2, 0.4$ and 0.6):

Compound	Pt.	La	Ba	Ni	Compound	Pt.	La	Ba	Ni
La_2NiO_4	1	64.72	--	35.28	$\text{La}_{1.8}\text{Ba}_{0.2}\text{NiO}_4$	1	60.40	6.66	32.94
	2	66.53	--	33.47		2	60.90	7.01	32.09
	3	66.71	--	32.71		3	60.12	6.75	33.13
	4	68.83	--	30.55		4	61.03	6.78	32.19
	5	66.93	--	33.07		5	61.05	6.45	32.50
AVG.		66.74	--	33.02		60.70	6.73	32.57	
EXPECTED VALUES		66.67	--	33.33		60.00	6.67	33.33	
$\text{La}_{1.6}\text{Ba}_{0.4}\text{NiO}_4$	1	54.74	12.63	32.64	$\text{La}_{1.4}\text{Ba}_{0.6}\text{NiO}_4$	1	47.24	19.82	32.94
	2	54.19	12.11	33.70		2	47.08	19.05	33.87
	3	54.09	12.66	33.25		3	47.35	19.79	32.86
	4	54.28	12.78	32.95		4	47.00	19.22	33.77
	5	55.79	12.92	31.29		5	46.78	20.52	32.70
AVG.		54.62	12.62	32.77		47.89	19.68	33.23	
EXPECTED VALUES		53.33	13.33	33.33		46.67	20.00	33.33	

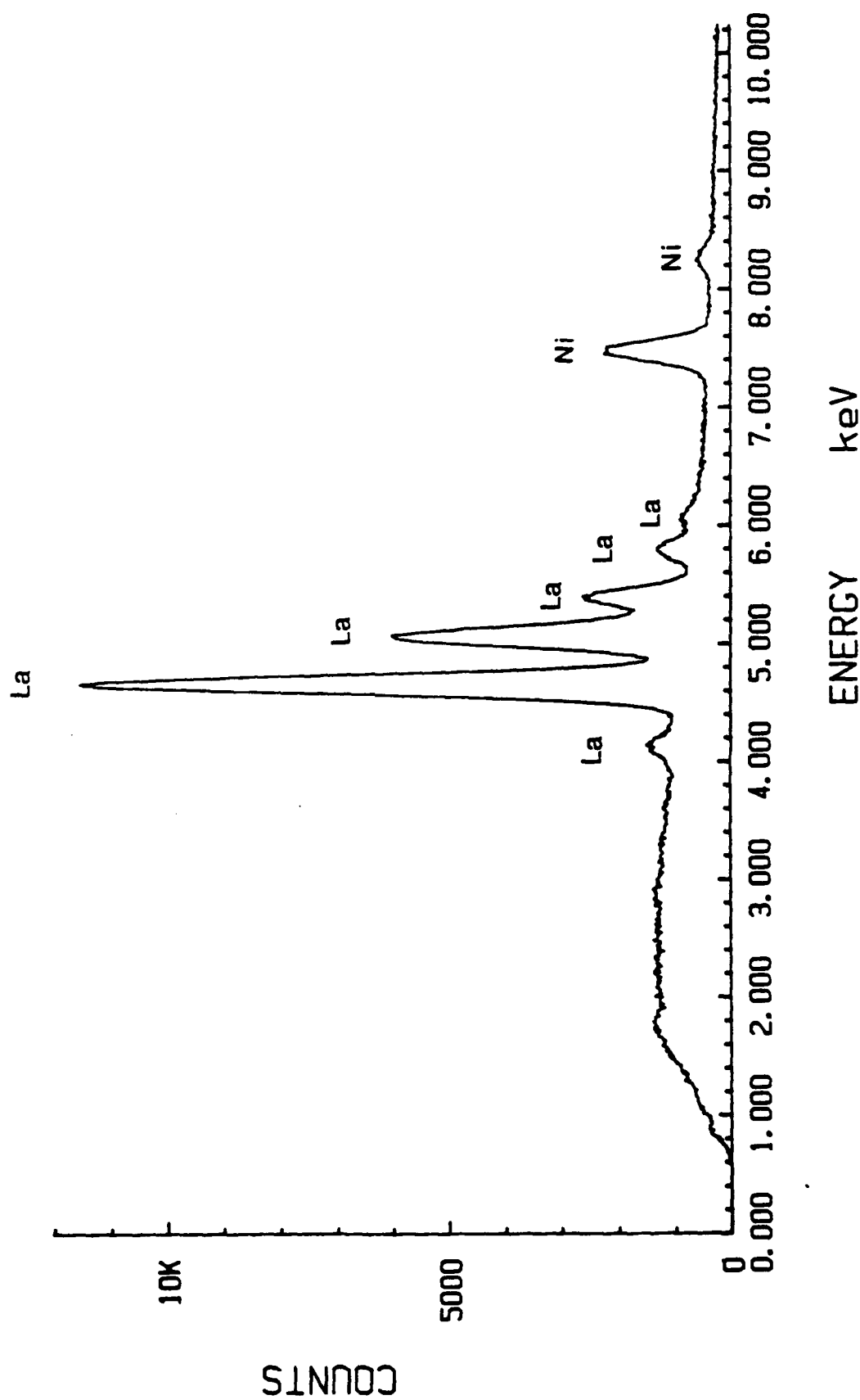


Figure 3.6. Microchemical analysis of La_2NiO_4 . The La l lines and Ni k lines are indicated.

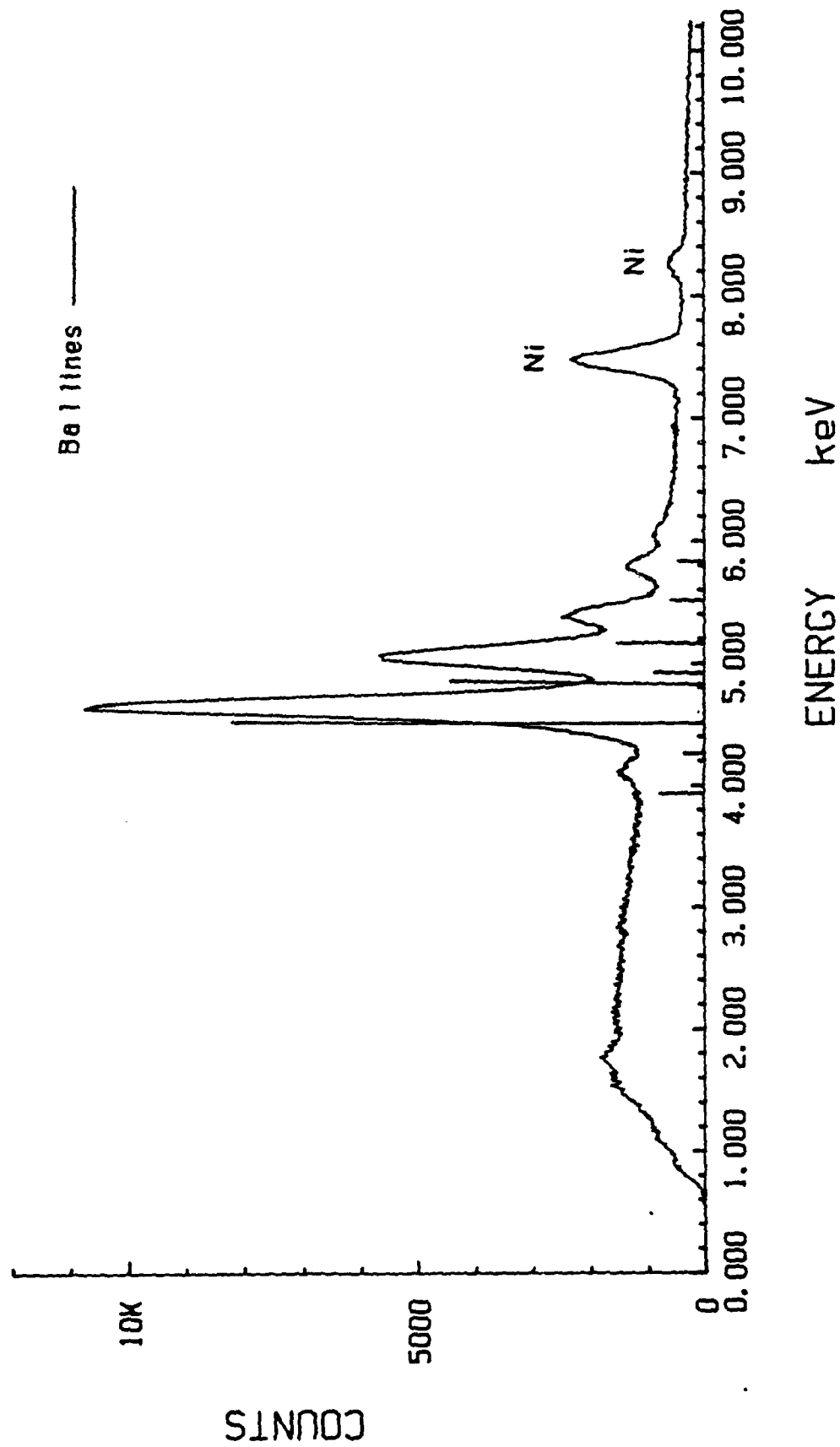


Figure 3.7. Microchemical analysis of $\text{La}_{1.8}\text{Ba}_{0.2}\text{NiO}_4$. The Ba 1 lines overlap with those of La, so a program is used to deconvolute the peaks.

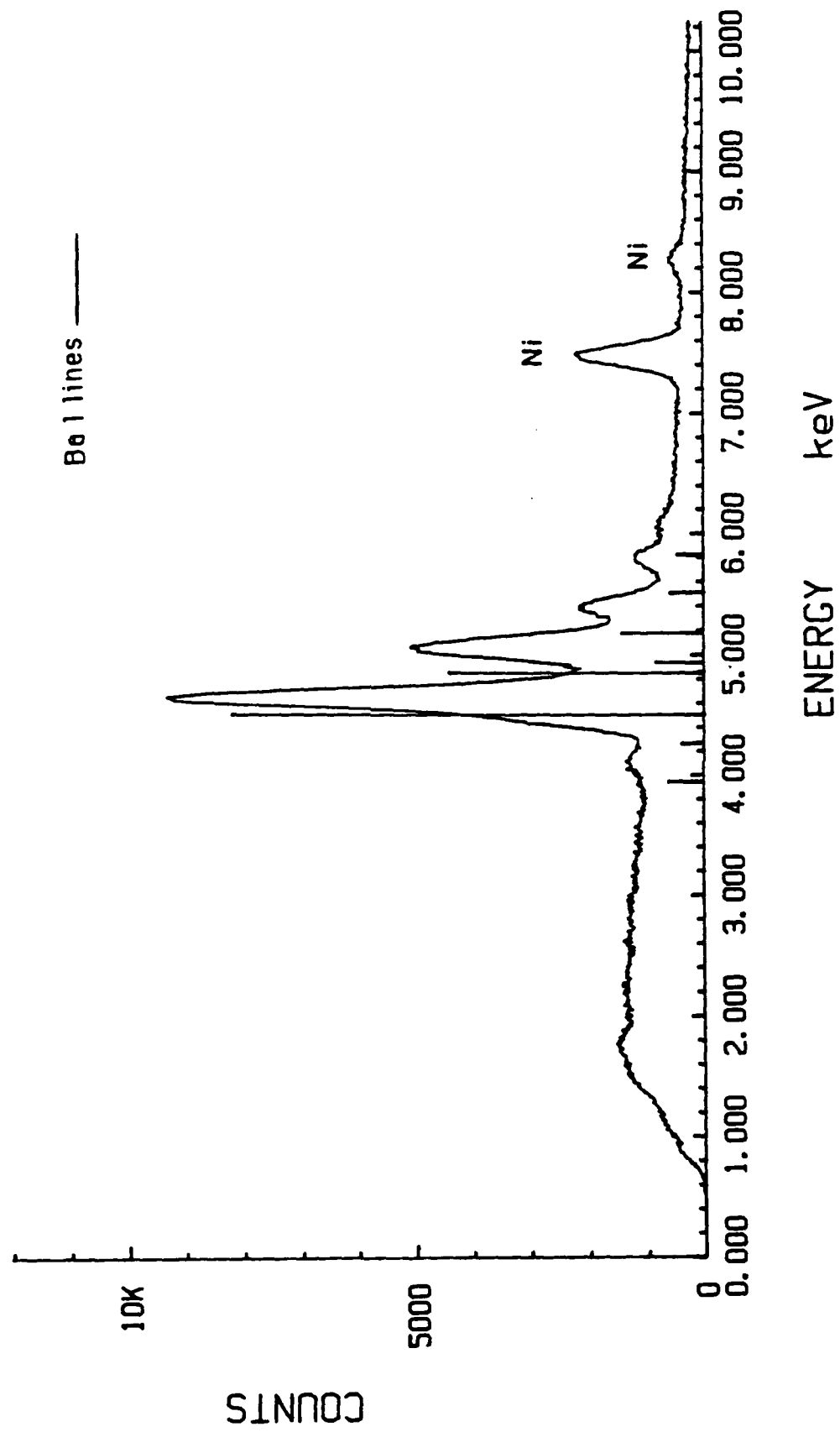


Figure 3.8. Microchemical analysis of $\text{La}_{1.6}\text{Ba}_{0.4}\text{NiO}_4$.

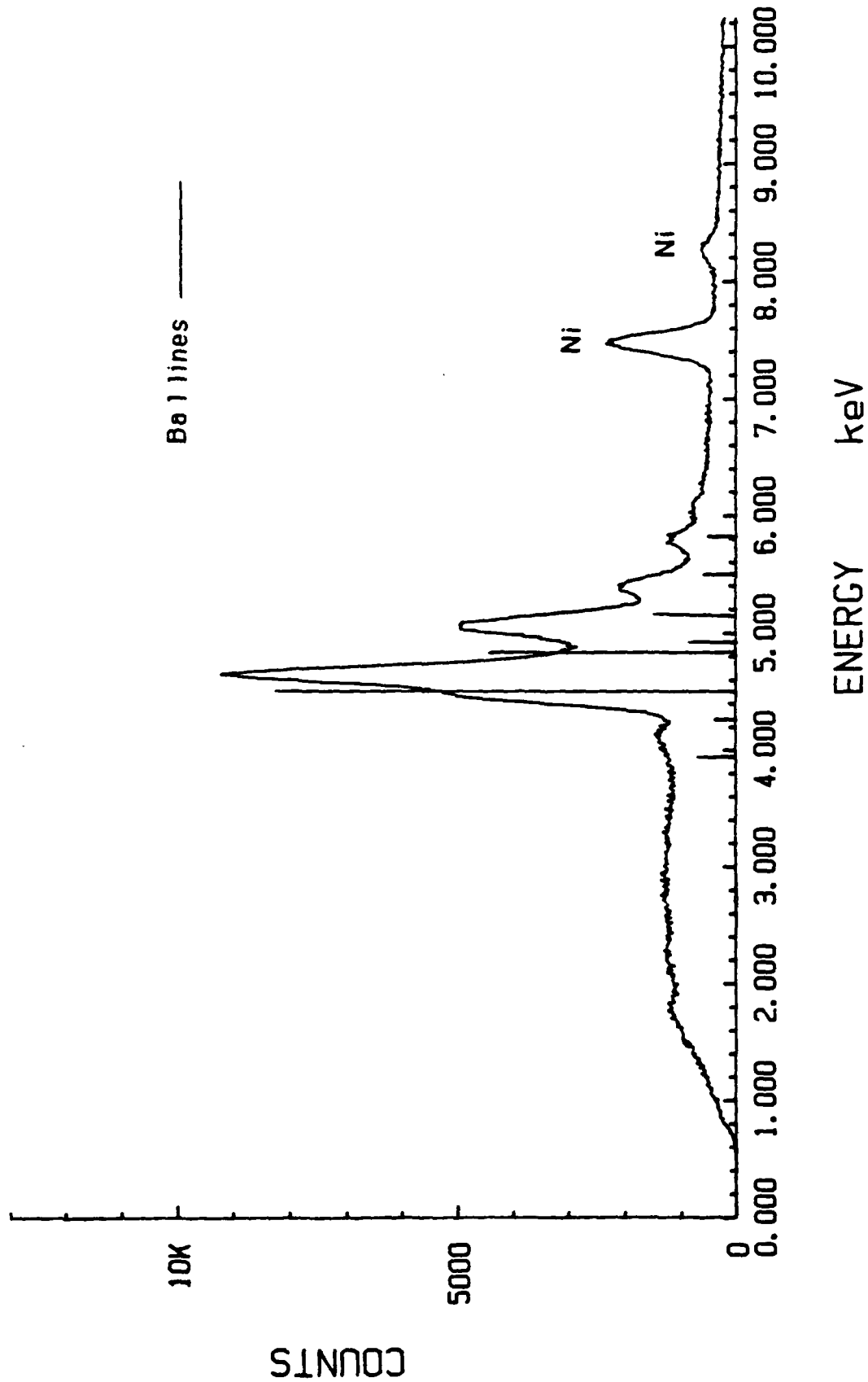


Figure 3.9. Microchemical analysis of $\text{La}_{1.4}\text{Ba}_{0.6}\text{NiO}_4$. Due to the higher concentration of Ba in this sample, the Ba lines become more distinct from those of La as evidenced by the shoulder formed on the left side of the strongest La peak.

Iodometric titrations²⁹ were also performed on La_2NiO_4 to determine oxygen stoichiometry by measuring the Ni^{3+} content. The end point of these titrations was unable to be determined accurately due to the presence of a precipitate in the solution. The titrations did indicate, however, that Ni^{3+} was present in the compound.

Many others^{5-7,21,30} have reported an excess of oxygen in both polycrystalline and single crystal La_2NiO_4 when prepared in ambient conditions. In addition, oxygen excesses have been reported for the analogous system $\text{La}_{2-x}\text{Sr}_x\text{NiO}_4$ in the range ($0 \leq x \leq 0.6$), with the amount of excess oxygen decreasing with increasing concentration of strontium.²¹ (The compositions with higher strontium concentrations ($0.6 < x \leq 1.0$) were determined to be stoichiometric.) In all of these cases, the oxygen excess is attributed to the presence of Ni^{3+} in the compound. From 3 up to as much as 20% Ni^{3+} has been reported for La_2NiO_4 samples prepared under ambient conditions.^{6,7} As high as 32% Ni^{3+} has been reported for La_2NiO_4 crystals which were melted and grown under a continuous flow of pure oxygen.³⁰ When grown under these high oxygen partial pressures (80 - 100%), the crystals showed extensive cracking.

Ganguly and Rao⁸ propose that the oxidation of Ni^{2+} to Ni^{3+} occurs in order to lower the energy of the system by stabilizing the tetragonal K_2NiF_4 structure. According to equation 2-1 the tetragonal K_2NiF_4 structure is stable within the limits $0.85 \leq t \leq 1.02$ and most stable for t equal to 1.0, where t is the ratio of bond lengths $\frac{\sqrt{2}}{2}(A - O - A)/(B - O - B)$. For La_2NiO_4 t is equal to 0.876, which is at the lower limit of stability. If Ni^{2+} were to be oxidized to Ni^{3+} , however, the $B - O - B$ distance would decrease, causing t to increase and making

the structure more stable.* This explanation -- that excess Ni^{3+} stabilizes the tetragonal structure -- is substantiated by the fact that when La_2NiO_4 is stoichiometric or slightly oxygen deficient (i.e. no Ni^{3+} is present) it is unable to support the tetragonal structure; the NiO_6 octahedra are forced to tilt along the $\langle 110 \rangle$ direction, so that La_2NiO_4 possesses a monoclinic structure.^{6,8}

The fact that the oxygen excess lessens with increasing barium substitution in the present system (and also with strontium substitution in $\text{La}_{2-x}\text{Sr}_x\text{NiO}_4$, as reported in the literature) is to be expected, as the substitutions create an increasing amount of Ni^{3+} ; thus t increases automatically with divalent cation substitution, so less oxygen-excess is needed in these compositions to achieve the same degree of structural stability achieved with greater oxygen excesses in samples of lower barium (or strontium) content.

In the present work, a high amount of Ni^{3+} exists in the La_2NiO_4 sample (26%), as compared to what others have reported (3-20%). This can be attributed to the nitration precursor process initially producing the higher oxidation state of nickel (Ni^{3+}), which remains stable to temperatures much higher than that at which the nitrates burn off. As the oxides begin to react, forming La_2NiO_4 , the Ni^{3+} stabilizes the tetragonal cell structure, so that very little of the oxidized Ni^{3+} is ever allowed to reduce back to Ni^{2+} , and its presence causes there to be an oxygen excess in order to maintain charge balance.

Possibilities have been suggested to account for the presence of the excess oxygen in the structure. Drennan *et al.*³¹ propose that in La_2NiO_4 there may exist intergrowths of the Ruddlesden-Popper³² type phases $\text{La}_3\text{Ni}_2\text{O}_7$ and $\text{La}_4\text{Ni}_3\text{O}_{10}$.

* Furthermore, if the Ni^{3+} ions exist in the low-spin state, as they do in the present system, the energy of the system may be lowered even further if the Jahn-Teller distortion puts the B - O - B bond into compression.

Such intergrowths would be possible if the Ni^{3+} ions were to be randomly distributed, causing the LaNiO_3 layer to be electrically neutral. High resolution electron microscopy (HREM) has been performed on oxygen-excess La_2NiO_4 prepared by two different groups^{30,33}, however, with no evidence for these higher-order phases being found. Another explanation for the presence of excess oxygen in the structure is A-site deficiency.

3.4 Magnetic Susceptibility Measurements

The magnetic susceptibilities for $\text{La}_{2-x}\text{Ba}_x\text{NiO}_4$ ($x = 0, 0.2, 0.4$ and 0.6) as a function of temperature are shown in Fig. 3.10. These measurements were performed on a SQUID magnetometer. The magnetic susceptibility for La_2NiO_4 was also measured using the Faraday method. Figure 3.11 shows the two measurements of La_2NiO_4 to be in good agreement.

Both of the measurements show an anomaly in the La_2NiO_4 susceptibility curve at 110 K. A similar anomaly was seen by Buttrey *et al.*⁶ in a single crystal $\text{La}_2\text{NiO}_{4.10}$ sample and also in $\text{La}_2\text{NiO}_{4+\delta}$ ($\delta > 0$) powders, while others have noted discontinuities in Curie-Weiss law plots for $\text{La}_2\text{NiO}_{4+\delta}$ ($\delta > 0$).^{3,8,34} This anomalous behavior is not well understood, but appears to be indicative of oxygen-excess $\text{La}_2\text{NiO}_{4+\delta}$. As δ goes to zero, the anomaly disappears, with the susceptibility becoming almost temperature independent. Studies done on single crystals of nearly stoichiometric $\text{La}_2\text{NiO}_{4.005}$ and $\text{La}_2\text{NiO}_{4.000}$ show them to exhibit long-range quasi-two-dimensional antiferromagnetic order, with the slightly oxygen-excess sample having broad transitions from isotropic to anisotropic susceptibility near 100 and 250 K.⁶

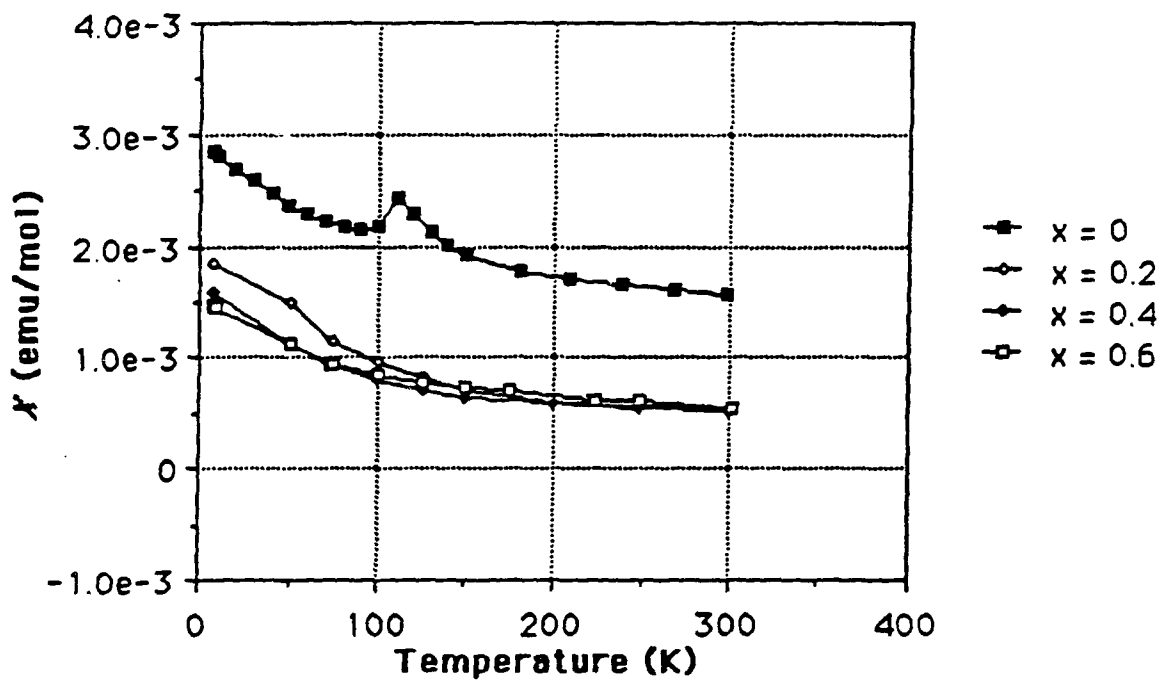


Figure 3.10 Magnetic susceptibility as a function of temperature and barium concentration in $\text{La}_{2-x}\text{Ba}_x\text{NiO}_4$ ($x = 0, 0.2, 0.4$ and 0.6). An anomaly in the susceptibility curve is present for La_2NiO_4 . This anomaly disappears and the magnetic susceptibility drops significantly with the addition of barium into the system.

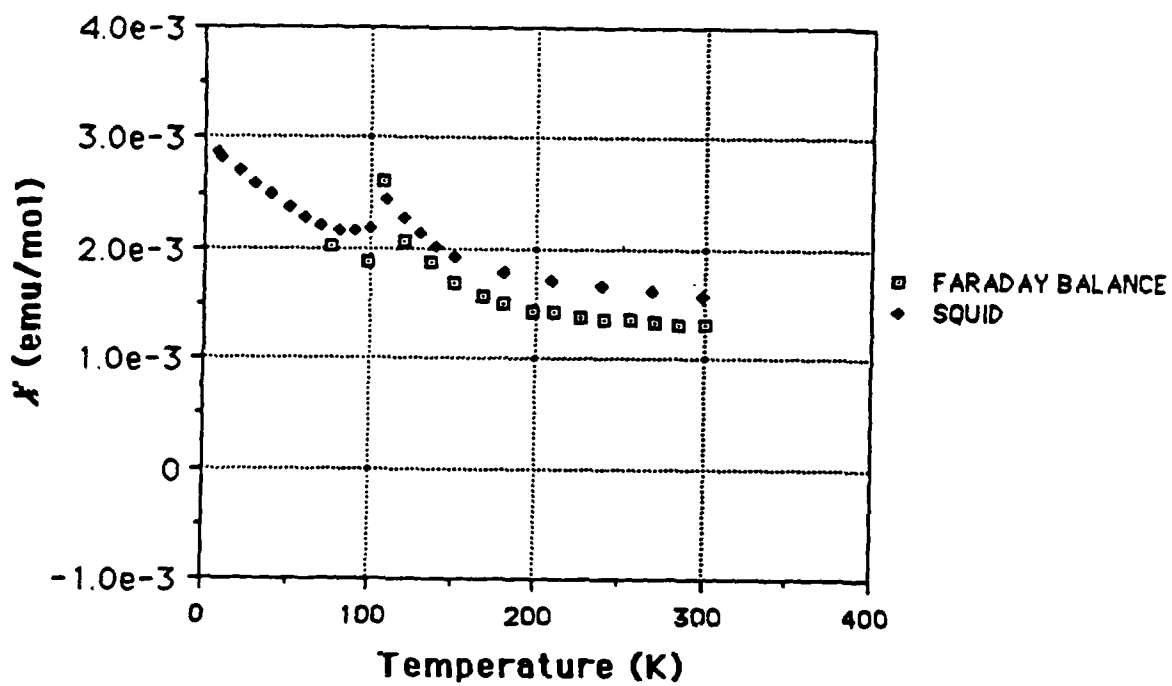


Figure 3.11 Magnetic susceptibility versus temperature for La_2NiO_4 measured using a Faraday balance (\square) and a SQUID magnetometer (\blacklozenge).

Although the transitions from isotropic to anisotropic behavior are still not well-understood, Buttrey *et al.*⁶ explain the antiferromagnetic ordering in terms of the monoclinic structure of stoichiometric La_2NiO_4 . In this structure the nearest neighbor NiO_6 octahedra are tilted in opposite directions away from the c -axis in the (001) plane. This tilting of octahedra removes the inversion center which would otherwise be present between nearest-neighbor Ni sites, thereby allowing spin canting as a result of the Dzialoshinskii-Moriya antisymmetric superexchange interaction.^{35,36}

Even in oxygen-excess $\text{La}_2\text{NiO}_{4+\delta}$ ($\delta > 0$) there may be slight tilting of the NiO_6 octahedra at low temperatures, which could be responsible for the observed anomaly. Singh *et al.*³⁴ found the c/a ratio of $\text{La}_2\text{NiO}_{4+\delta}$ ($\delta > 0$) to decrease with decreasing temperature over the temperature range of 773 to 77 K. This means that as $\text{La}_2\text{NiO}_{4+\delta}$ is cooled below room temperature the $\frac{\sqrt{2}}{2}$ (La - O - La) bond length may continue to elongate until the tetragonal structure becomes unstable, with tilting of the NiO_6 octahedra resulting. Buttrey *et al.*⁶ see an anomaly for $\text{La}_2\text{NiO}_{4.10}$ (20% Ni^{3+}) at 155 K, while in the present work similar behavior is seen at 110 K for $\text{La}_2\text{NiO}_{4.13}$ (26% Ni^{3+}). This implies that the temperature at which the anomaly occurs may be dependent on the amount of Ni^{3+} . This is reasonable if, in fact, the anomaly is somehow a manifestation of a distorted lattice. As already noted, Ni^{3+} helps to stabilize the tetragonal structure.⁷ Therefore, the tetragonal structure of the sample with the higher concentration of Ni^{3+} will be more stable at room temperature, and, most likely, continue to be stable down to

* Through TGA they determined that the oxygen content of their samples remained constant over the entire range of temperatures 300 - 800 K.

** Theoretically, there can not be too much Ni^{3+} in $\text{La}_2\text{NiO}_{4+\delta}$ because t , the stability factor, is closest to unity for the case of 100% Ni^{3+} .

lower temperatures than the sample containing less Ni^{3+} . Another way to look at it is the sample with the higher Ni^{3+} content will have a higher c/a ratio for a given temperature, as the Ni^{3+} , d^7 ion induces a Jahn-Teller distortion, which causes elongation in the c -direction and compression in the a - b plane. So, if there is a minimum c/a ratio, below which the tetragonal structure is no longer stable, the sample containing less Ni^{3+} should reach it at a higher temperature than the sample containing more Ni^{3+} . If the Ni^{3+} concentration is sufficiently high, the tetragonal structure should remain stable even down to extremely low temperatures, and no anomaly in the susceptibility curve should be observed.

With the substitution of 0.2 barium into the system, the anomaly disappears and the overall susceptibility drops by a factor of approximately one-third. With further increases in barium, a slight decrease in susceptibility is noted in the temperature range 6 to 50 K; for higher temperatures the susceptibility values did not differ significantly among any of the Ba-substituted compounds. The disappearance of the anomaly with the introduction of barium into the system can be attributed to the increased amount of Ni^{3+} for two possible reasons. First, the increased amount of Ni^{3+} may be enough to maintain the stability of the tetragonal structure down to 6 K. Second, the increased ferromagnetic interactions due to the higher concentration of Ni^{3+} ions might suppress the magnetic ordering present in the $\text{La}_2\text{NiO}_{4+x}$ sample, and, thus, cause the disappearance of the anomaly.⁶

An attempt was made to fit the data of Fig 3.10 to a Curie-Weiss law. (See Appendix D.) The La_2NiO_4 sample conforms to Curie-Weiss behavior above the reported anomaly (in the temperature range 180 to 300 K). Below the said anomaly, it once again conforms to Curie-Weiss behavior (in the temperature range 6 to 70 K). The Ba-substituted samples were fit to a Curie-Weiss law for the temperature range 50 to 200 K. The calculated Curie constants, C_m , Weiss

Table 3.3 Magnetic constants derived from the Curie-Weiss law for the compositional series $\text{La}_{2-x}\text{Ba}_x\text{NiO}_4$ ($x = 0, 0.2, 0.4$ and 0.6):

Compound	Temp. Range of fit (K)	C (emu ^o K/mol)	μ_{eff} (μ_{B} /Ni ion)	θ_{c} (K)	S
$\text{La}_2\text{NiO}_{4.13}$	6 - 70	0.61	2.21	-338	0.71
$\text{La}_2\text{NiO}_{4+\delta}$ ($\delta > 0$) ³⁴	< 200	0.42	1.83	-117	0.54
$\text{La}_2\text{NiO}_{4.13}$	200 - 300	1.66	3.65	-458	1.39
$\text{La}_2\text{NiO}_{4+\delta}$ ($\delta > 0$) ³⁴	200 - 300	1.15	3.03	-500	1.10
$\text{La}_2\text{NiO}_{4+\delta}$ ($\delta > 0$) ³	200 - 300	1.84	3.84	-500	1.48
$\text{La}_{1.8}\text{Ba}_{0.2}\text{NiO}_4$	50 - 200	0.15	1.08	-347	0.24
$\text{La}_{1.6}\text{Ba}_{0.4}\text{NiO}_4$	50 - 200	0.17	1.18	-647	0.27
$\text{La}_{1.4}\text{Ba}_{0.6}\text{NiO}_4$	50 - 200	0.24	1.39	-740	0.36

$$\mu_{\text{eff}} = [4S(S+1)]^{0.5} \mu_{\text{B}}$$

constant, θ_c , effective magnetic moments, μ_{eff} , and spins, S , for these compositions are given in Table 3.3, along with some of the reported values for oxygen-excess $\text{La}_2\text{NiO}_{4+\epsilon}$ samples.

The high-temperature fit for $\text{La}_2\text{NiO}_{4.13}$ yields a μ_{eff} of $3.65 \mu_{\text{B}}/\text{Ni}$ ion, which is higher than the spin-only value of $2.83 \mu_{\text{B}}/\text{Ni}$ ion for an $S = 1$ system. Likewise, the low-temperature fit gives a μ_{eff} of $2.21 \mu_{\text{B}}/\text{Ni}$ ion, which is higher than the spin-only value of $1.73 \mu_{\text{B}}/\text{Ni}$ ion for an $S = 1/2$ system and less than that for an $S = 1$ system. The magnetic data suggests the system can not be interpreted on the basis of spin-only moments. The fact that the Weiss constant for $\text{La}_2\text{NiO}_{4.13}$ is large and negative, however, is consistent with the existence of antiferromagnetic coupling.³⁴ In addition, based on Goodenough's^{34,22} model of conduction in La_2NiO_4 (which will be addressed in more detail in the following section), the observed μ_{eff} 's obtained from a conventional Curie-Weiss law should be higher than the theoretical value of μ_{eff} , with the magnetic susceptibility only approaching a localized-electron Curie-Weiss behavior at very high temperatures. This is true for all of the La_2NiO_4 μ_{eff} values in Table 3.3, although the high- and low-temperature μ_{eff} 's obtained on the $\text{La}_2\text{NiO}_{4+\epsilon}$ ($\epsilon > 0$) sample of Singh *et al.*³⁴ are only slightly greater than the μ_{eff} 's corresponding to an $S = 1$ and an $S = 1/2$ system, respectively.

In the case of the Ba-substituted samples, possibly less can be said about the data because of the limited range of temperatures over which the Curie-Weiss law could be fit. There is a sharp drop in C_m with the substitution of barium into the system, after which C_m did not change significantly with increasing barium. The value of C_m in the Ba-substituted samples corresponds to an approximate μ_{eff} of

$1.22 \pm 0.16 \mu_B$. This drop in μ_{eff} can be attributed to a partial delocalization of electrons caused by the increased concentration of Ni^{3+} ions in $\text{La}_{2-x}\text{Ba}_x\text{NiO}_4$.

3.5 Electrical Resistivity Measurements

The room temperature electrical resistivities for $\text{La}_{2-x}\text{Ba}_x\text{NiO}_4$ ($x = 0, 0.2, 0.4$ and 0.6) are plotted in Fig. 3.12. A significant drop in resistivity, from 0.14 to $0.05 \Omega\text{-cm}$, is seen with the first substitution of barium into the system, and there is a gradual decrease in resistivity for further additions of barium. In addition, upon cooling, all of the compounds exhibited an increase in resistivity with decreasing temperature, indicative of semiconducting behavior.

The decrease in electrical resistivity with the initial substitution of barium for lanthanum can be attributed to a $\text{Ni}^{2+}/\text{Ni}^{3+}$ mixed valence. This decrease is consistent with the drop in μ_{eff} upon barium substitution, which can be attributed to a partial delocalization of electrons caused by an increase in concentration of Ni^{3+} . This drop in both the resistivity and μ_{eff} is better understood by looking at the conduction model developed for La_2NiO_4 by Goodenough *et al.*^{34,22} As discussed in section 3.1, for La_2NiO_4 the Ni - O - Ni bond is in compression due to the pressure put on it by the alternating rock-salt layer. In addition, for $\text{La}_2\text{NiO}_{4+\delta}$ ($\delta > 0$) Ni^{3+} , d^7 ions are present and induce a Jahn-Teller distortion that serves to put even greater compression on the Ni - O - Ni bond. As it is the nickel 3d bands which determine the transport and magnetic properties of La_2NiO_4 ²², this model proposes that the strong pressure on the Ni - O - Ni bond causes intra-atomic exchange coupling with the localized d_{z^2} electrons to create narrow itinerant $\sigma_{x^2-y^2}$ bands in the a - b plane and a relative stabilization of the d_{z^2} orbitals along the c -axis. This causes enhanced

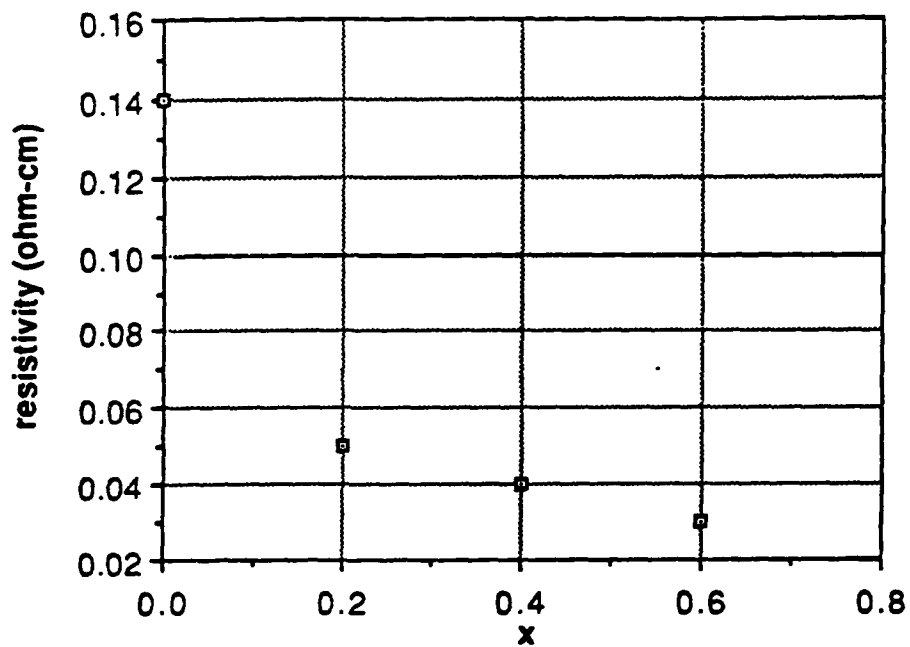


Figure 3.12 Electrical resistivity as a function of barium concentration in $\text{La}_{2-x}\text{Ba}_x\text{NiO}_4$ ($x = 0, 0.2, 0.4$ and 0.6). A significant decrease in resistivity is seen with the initial substitution of barium into the system and is attributed to the $\text{Ni}^{2+}/\text{Ni}^{3+}$ mixed valence state.

conduction in the a - b plane, which accounts for the low resistivity of $\text{La}_2\text{NiO}_{4+\delta}$.^{*} The above model applies to oxygen-excess $\text{La}_2\text{NiO}_{4+\delta}$; for stoichiometric La_2NiO_4 , the model predicts that the electrons remain localized. This is because for stoichiometric La_2NiO_4 the pressure normally put on the Ni - O - Ni bond by the rock-salt layer is removed by the tilting of the NiO_6 octahedra; and, interestingly enough, reported resistivities⁷ for stoichiometric La_2NiO_4 are three orders of magnitude higher than that which have been reported for some $\text{La}_2\text{NiO}_{4+\delta}$ samples.^{**}

It is the belief of the author that the additional compression put onto the Ni - O - Ni bond due to the substitution of 0.2 barium for lanthanum in La_2NiO_4 enhances the intra-atomic exchange coupling, increasing the number of itinerant electrons in the $\sigma_{x^2-y^2}$ bands, and, thus, causing both a decrease in resistivity and in μ_{eff} . The fact that neither of these parameters demonstrate a real change with further additions of barium indicates that a critical compression of the Ni - O - Ni bond is achieved with a barium concentration $x = 0.2$ in $\text{La}_{2-x}\text{Ba}_x\text{NiO}_4$. The additional compression put on the Ni - O - Ni bond due to subsequent substitutions of barium apparently does not enhance the intra-atomic exchange coupling; therefore, no notable change takes place in either the magnetic or transport properties.

* Because of the largely two-dimensional nature of the system $\text{La}_{2-x}\text{Ba}_x\text{NiO}_4$, the orientation-averaged electrical resistivity of a polycrystalline sample is essentially a measure of the resistivity in the a - b plane.

** Reported resistivities for $\text{La}_2\text{NiO}_{4+\delta}$ show the resistivity to decrease as δ increases.⁷

4. Conclusions and directions for future work

In summary, a compositional series $\text{La}_{2-x}\text{Ba}_x\text{NiO}_4$ ($0 \leq x \leq 1.0$) has been made by standard ceramic techniques, employing the use of nitrate precursors. After a low-temperature "pre-fire" to burn off the nitrates, single phase materials were achieved in two to three heatings at 1100°C , a reaction temperature 100°C lower than what is typically reported for La_2NiO_4 . All of the members of the compositional series were determined to possess a tetragonal K_2NiF_4 structure. In the case of La_2NiO_4 , it appears the presence of Ni^{3+} in the compound helps to stabilize the tetragonal structure, with its actual stoichiometry being $\text{La}_2\text{NiO}_{4.13}$. The exact stoichiometry of the $\text{La}_{1.4}\text{Ba}_{0.6}\text{NiO}_4$ sample was also determined, with it, too, having a slight excess of Ni^{3+} ($\text{La}_{1.4}\text{Ba}_{0.6}\text{NiO}_{4.08}$). Additional TGA should be done in order to determine the exact stoichiometries of all of the compounds. Gopalakishnan *et al.* saw an excess of oxygen in the analogous system $\text{La}_{2-x}\text{Sr}_x\text{NiO}_4$ ($0 \leq x \leq 1.0$) up to $x = 0.6$; for greater concentrations of strontium the compounds were determined to be stoichiometric. It is possible that similar behavior will be found in the present system -- this should be further explored.

The cell parameters were also determined for all of the compositions. With increasing concentration of barium, c initially increases, while a decreases, with this trend reversing in the compositional range $0.5 \leq x \leq 0.6$. The ratio of lattice parameters, c/a , reaches a maximum at $x = 0.6$. The increase in c/a is attributed to a weak Jahn-Teller distortion due to octahedral site low-spin Ni^{3+} ions, while the other results can generally be explained by taking into account the geometry of both the perovskite and rock-salt layers and the changing size of the A-site ion due to barium substitution and the B-site ion due to oxidation of Ni^{2+} to Ni^{3+} . Preliminary experiments also suggest the existence of Ni^{4+} ions in the higher Ba-containing compounds, which could also explain some of the observed changes in lattice

parameters. Additional experiments are being done to more completely determine the presence of Ni^{4+} in these compounds.

Magnetic and electrical measurements were made on the samples $\text{La}_{2-x}\text{Ba}_x\text{NiO}_4$ ($x = 0, 0.2, 0.4$ and 0.6). The stoichiometry of $\text{La}_2\text{NiO}_{4.13}$ was shown to be a critical factor affecting both its magnetic and electrical properties. The anomaly seen in the magnetic susceptibility of $\text{La}_2\text{NiO}_{4.13}$ was attributed to a possible distortion of the NiO_6 octahedra at low temperature. Previously, this behavior has gone unexplained, so it would be interesting to pursue this idea further. This could possibly be done by heating samples of $\text{La}_2\text{NiO}_{4+\epsilon}$ under varying oxygen partial pressures to achieve varying ϵ 's, with emphasis on making a sample with ϵ very large. If the theory proposed is correct, the temperature at which the anomaly occurs in the magnetic susceptibility curve should decrease as ϵ increases and for ϵ very large it should completely disappear. Significant decreases in both the magnetic susceptibility and the room temperature resistivity were seen with the substitution of 0.2 barium for lanthanum in $\text{La}_2\text{NiO}_{4+\epsilon}$, while additional substitutions of barium did not notably alter either of these properties. The magnetic susceptibility data was fit to the Curie-Weiss law, and the change seen in μ_{eff} with increasing barium concentration was correlated to the change seen in resistivity with increasing barium concentration. The observed magnetic and electrical data was found to be consistent with the conduction model for La_2NiO_4 developed by Goodenough *et al.*^{34,22} There is much work which could still be done in the area of magnetic and electrical studies. It would be of interest to measure the electrical and magnetic properties for $\text{La}_{2-x}\text{Ba}_x\text{NiO}_4$ in the range $0.6 < x \leq 1.0$ and to correlate these properties with the cell parameters reported for those compositions in this work. Also of interest would be to study the temperature dependence of electrical resistivity in all of the compositions $\text{La}_{2-x}\text{Ba}_x\text{NiO}_4$ ($0 \leq x \leq 1.0$).

In respect, to high T_c superconductivity, it would also be interesting to stabilize Ni^{+} in La_2NiO_4 by 4+ cation or 1- anion substitution.* The aim being to create a system analogous to the high T_c superconductor, $La_{1.85}Sr_{0.15}CuO_4$, with both possessing the tetragonal K_2NiF_4 structure and a d^8 , d^9 electronic configuration. Attempts have already been made to substitute cerium for lanthanum in La_2NiO_4 , but single phase materials were not obtained. As monovalent nickel has scarcely been observed in mineral compounds, it is likely that this will be a difficult task. Recently, however, a pure monovalent nickel phase, $LaNiO_2$, has been reported,³⁸ which gives hope for eventual success in this effort.

Additional studies which are continuing on these materials have been spurred by reports of the unique absorption characteristics of $La_{2-x}Sr_xCuO_4$. A giant absorption of power from an *rf* field of ~1 GHz has been reported for both the semiconducting and metallic members of $La_{2-x}Sr_xCuO_4$. Absorptions of this magnitude are usually associated with metals, whose reflective properties often make it difficult to take advantage of their unique absorption characteristics. Therefore, the discovery of a semiconductor (La_2CuO_4) which possesses this quality is of great interest. All of the compositions $La_{2-x}Ba_xNiO_4$ ($0 \leq x \leq 1.0$) have demonstrated semiconducting behavior. If this present series of compositions possesses similar power absorption characteristics to the series $La_{2-x}Sr_xCuO_4$, it could prove to be very exciting; it would then be of interest to study the effect of structural, electronic and magnetic properties on *rf* power absorption for the system $La_{2-x}Ba_xNiO_4$.

* Initially, this was attempted by oxygen reduction of La_2NiO_4 ; but this is no longer believed to be the method to use, as this would be expected to monoclinically distort the lattice and the system $La_{2-x}M_xCuO_4$ ($M = Sr$ or Ba) is only superconducting when it possesses tetragonal symmetry.

Appendix A

A. Van der Pauw Method of Measuring Resistivity

L. J. van der Pauw has described a method of measuring resistivity of a lamella of arbitrary shape.^{39,40} The procedure was to select a flat lamella, completely free of holes, and provide it with four small contacts, M, N, O and P placed arbitrarily along the periphery. (Fig. A.1) A current i_{MN} was applied to contact M and taken off at contact N. The potential difference $V_P - V_O$ was measured and $R_{MN,OP}$ was obtained.

$$R_{MN,OP} = \frac{V_P - V_O}{i_{MN}} \quad (A-1)$$

and, similarly,

$$R_{NO,PM} = \frac{V_M - V_P}{i_{NO}} \quad (A-2)$$

The method of measurement is based on the theorem that between $R_{MN,PM}$ and $R_{NO,PM}$ there exists the simple relation:

$$\exp\left(\frac{-\pi d}{\rho} R_{MN,OP}\right) + \exp\left(\frac{-\pi d}{\rho} R_{NO,PM}\right) = 1, \quad (A-3)$$

where d is the thickness of the lamella and ρ is the resistivity of the material. If d and the "resistances" $R_{MN,OP}$ and $R_{NO,PM}$ are known, then (A - 3) yields an equation in which ρ is the only unknown quantity. The situation is particularly straightforward in the special case where the sample possesses a line of symmetry. In that case, M and O are placed on the line of symmetry, while N and P are disposed symmetrically with respect to the line. (Fig. A.2)

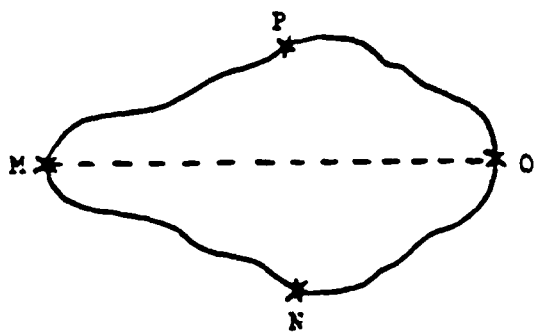


Figure A.1 Flat lamella of arbitrary shape showing contacts at points M, N, O and P.

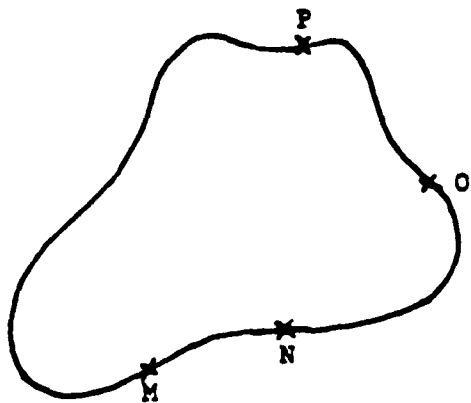


Figure A.2 Flat lamella having a line of symmetry showing contacts at M, N, O and P.

Then:

$$R_{NO,OP} = R_{MN,OP}. \quad (A-4)$$

and from (A - 3) it can easily be seen that

$$\rho = \frac{\pi d}{\ln 2} (R_{MN,OP}). \quad (A-5)$$

Thus, in this case a single measurement suffices.

In the general case it is not possible to express ρ explicitly in known functions. The solution can, however, be written in the form:

$$\rho = \frac{\pi d}{\ln 2} \left(\frac{R_{MN,OP} + R_{NO,PM}}{2} \right) f, \quad (A-6)$$

where f is a factor which is a function only of the ratio $R_{MN,OP}/R_{NO,PM}$ as plotted in Fig. A.3. Therefore, f is determined by calculating $R_{MN,OP}/R_{NO,PM}$ and then reading the corresponding value from Fig. A.3., and ρ is then calculated from (A-6).

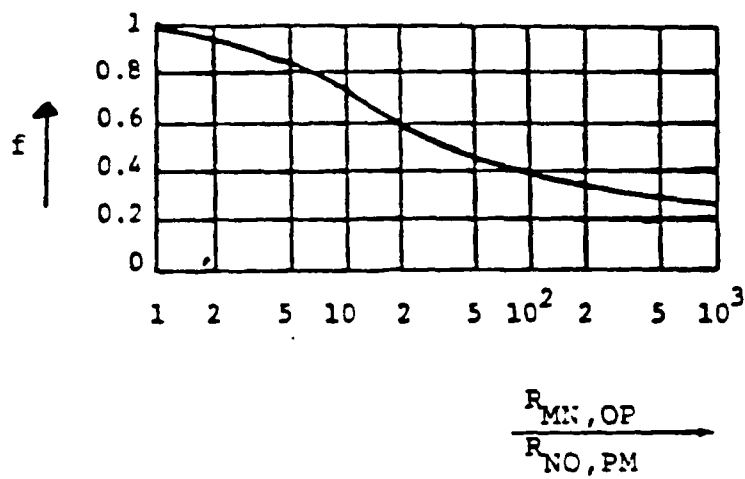


Figure A.3 Graphical representation of van der Pauw's f factor from:

$$\cosh \left[\frac{(R_{MN,OP}/R_{NO,PM})^{-1} \frac{\ln 2}{1}}{(R_{MN,OP}/R_{NO,PM})^{+1} \frac{\ln 2}{1}} \right] = \frac{1}{2} \exp \frac{\ln 2}{f}$$

Appendix B

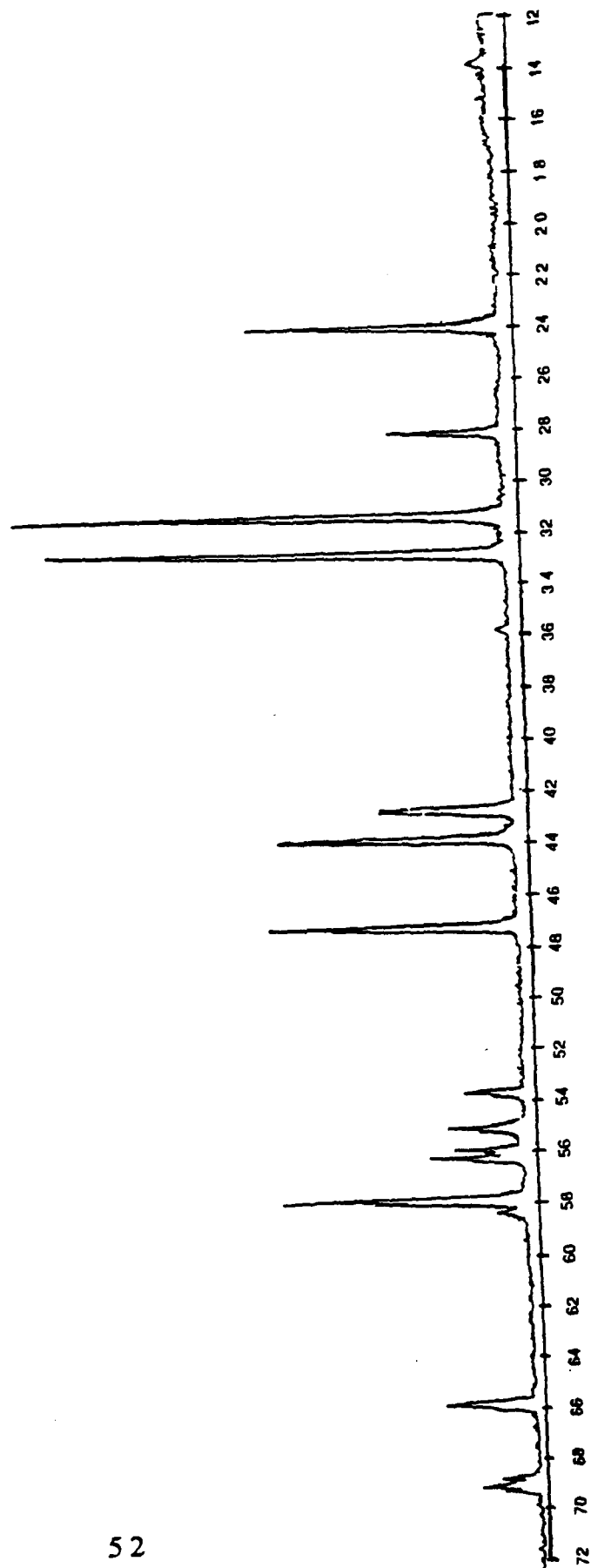


Figure B.1. X-ray diffraction pattern for La_2NiO_4 .

Appendix B (cont.)

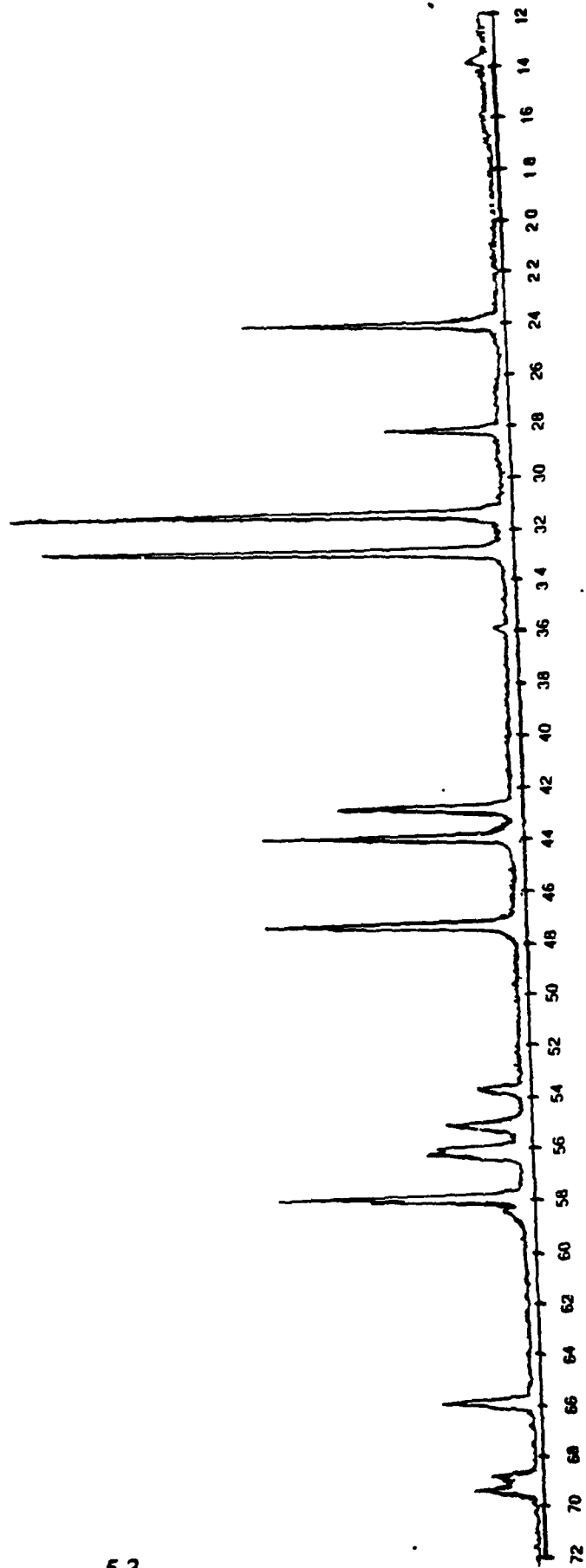


Figure B.2. X-ray diffraction pattern for $\text{La}_{1.9}\text{Ba}_{0.1}\text{NiO}_4$.

Appendix B (cont.)

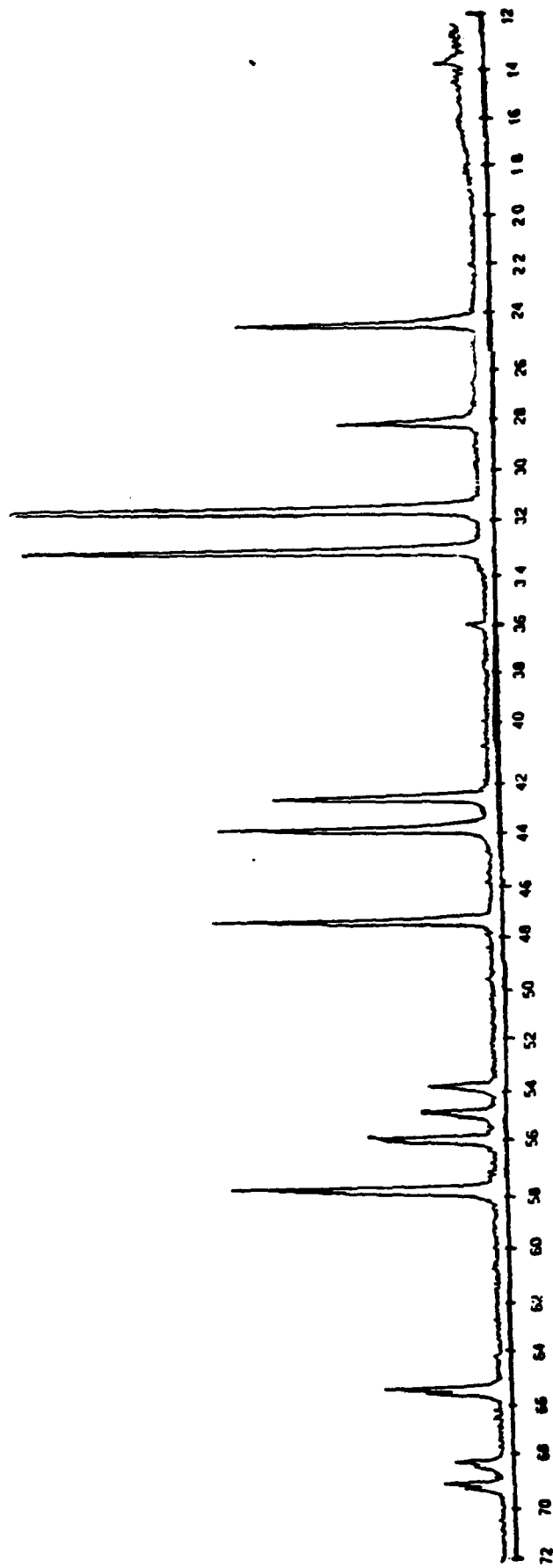


Figure B.3. X-ray diffraction pattern for $\text{La}_{1.8}\text{Ba}_{0.2}\text{NiO}_4$.

Appendix B (cont.)

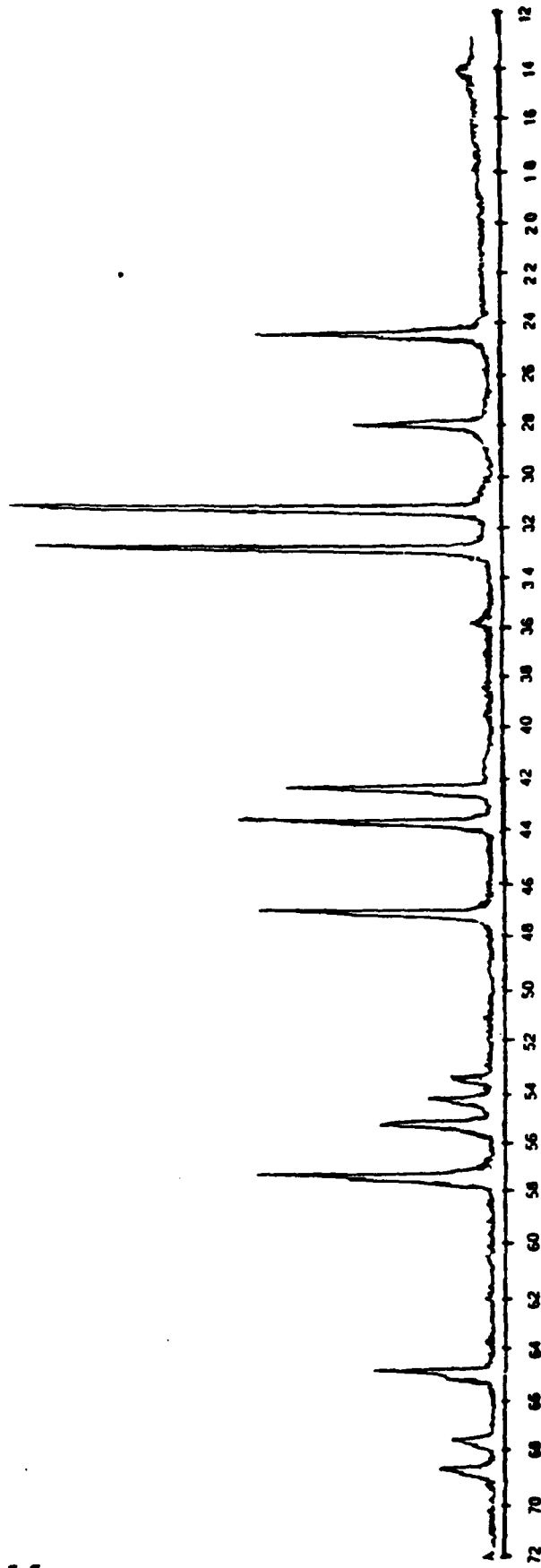


Figure B.4. X-ray diffraction pattern for $\text{La}_{1.7}\text{Ba}_{0.3}\text{NiO}_4$.

Appendix B (cont.)

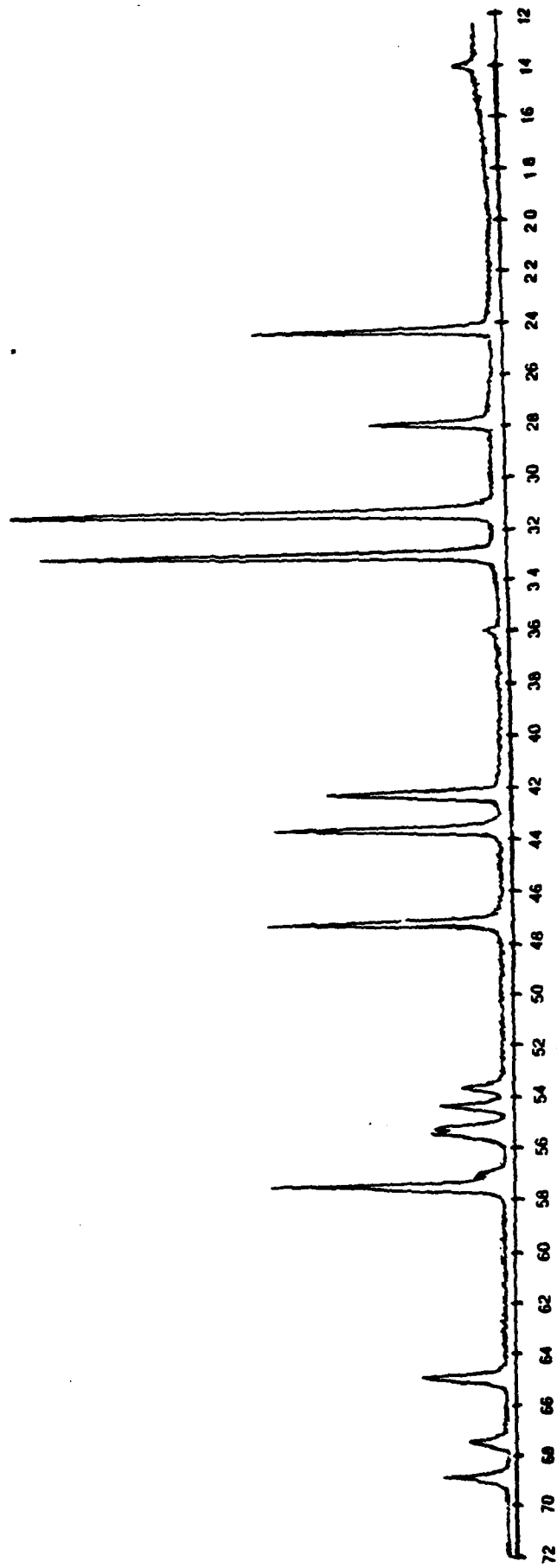


Figure B.5. X-ray diffraction pattern for $\text{La}_{1.6}\text{Ba}_{0.4}\text{NiO}_4$.

Appendix B (cont.)

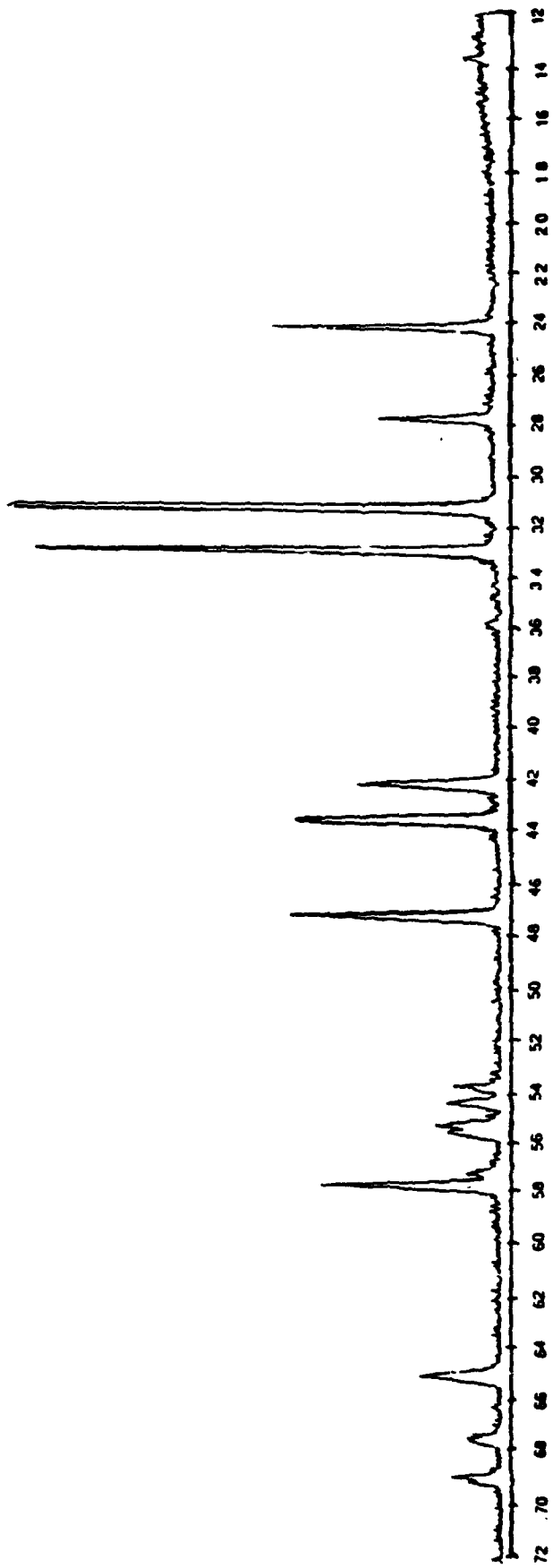


Figure B.6. X-ray diffraction pattern for $\text{La}_{1.5}\text{Ba}_{0.5}\text{NiO}_4$.

Appendix B (cont.)

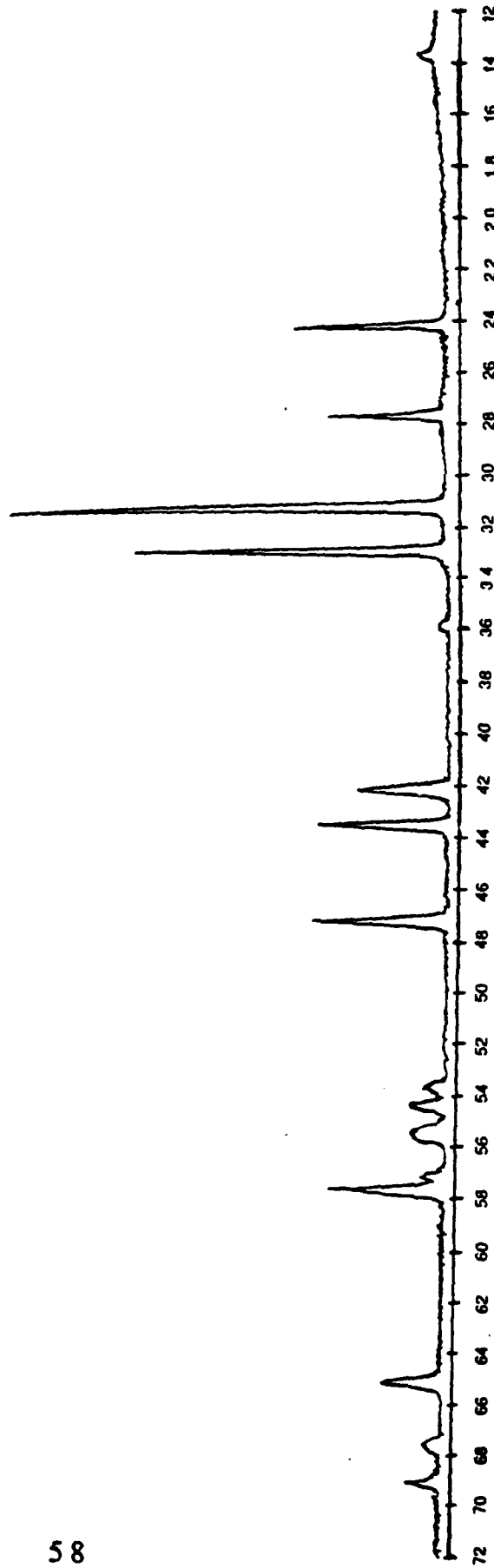


Figure B.7. X-ray diffraction pattern for $\text{La}_{1.4}\text{Ba}_{0.6}\text{NiO}_4$.

Appendix B (cont.)

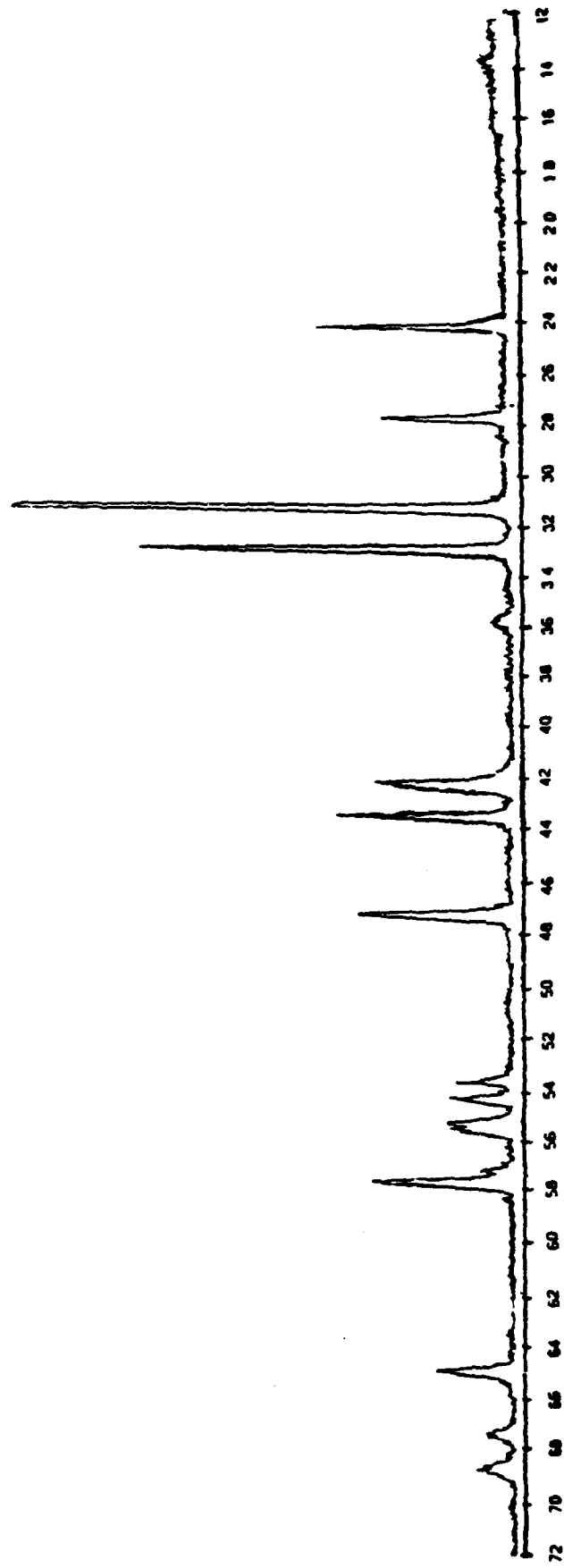


Figure B.6. X-ray diffraction pattern for $\text{La}_{1.3}\text{Ba}_{0.7}\text{NiO}_4$.

Appendix B (cont.)

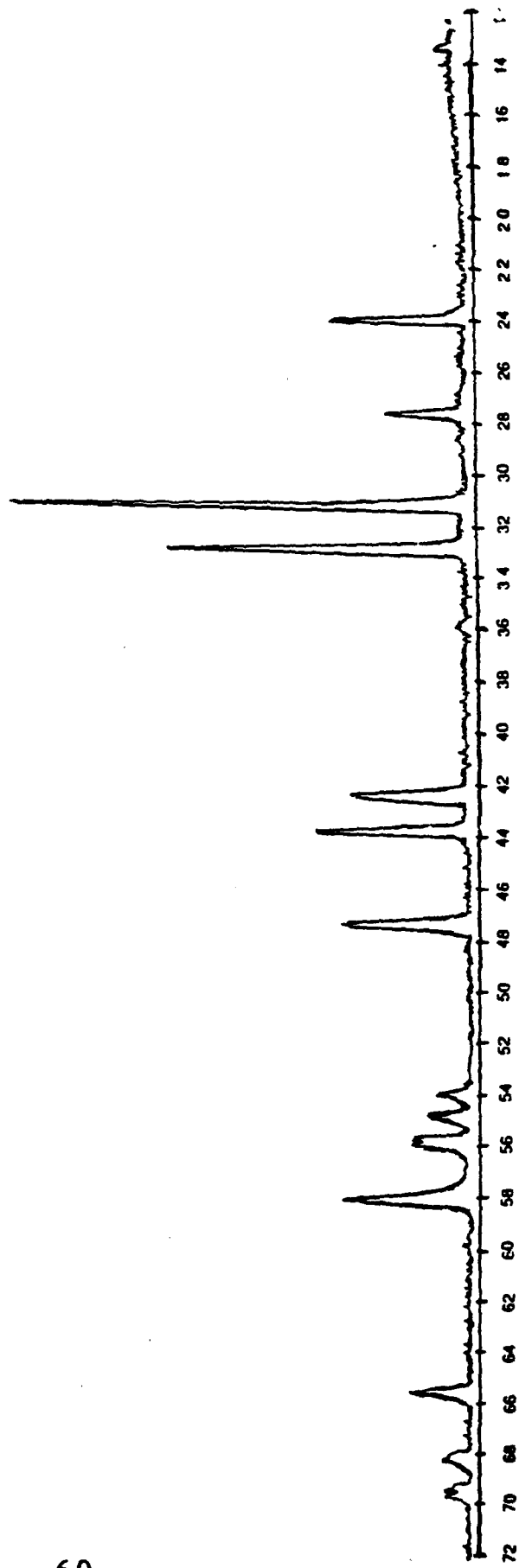


Figure B.9. X-ray diffraction pattern for $\text{La}_{1.2}\text{Ba}_{0.8}\text{NiO}_4$.

Appendix B (cont.)

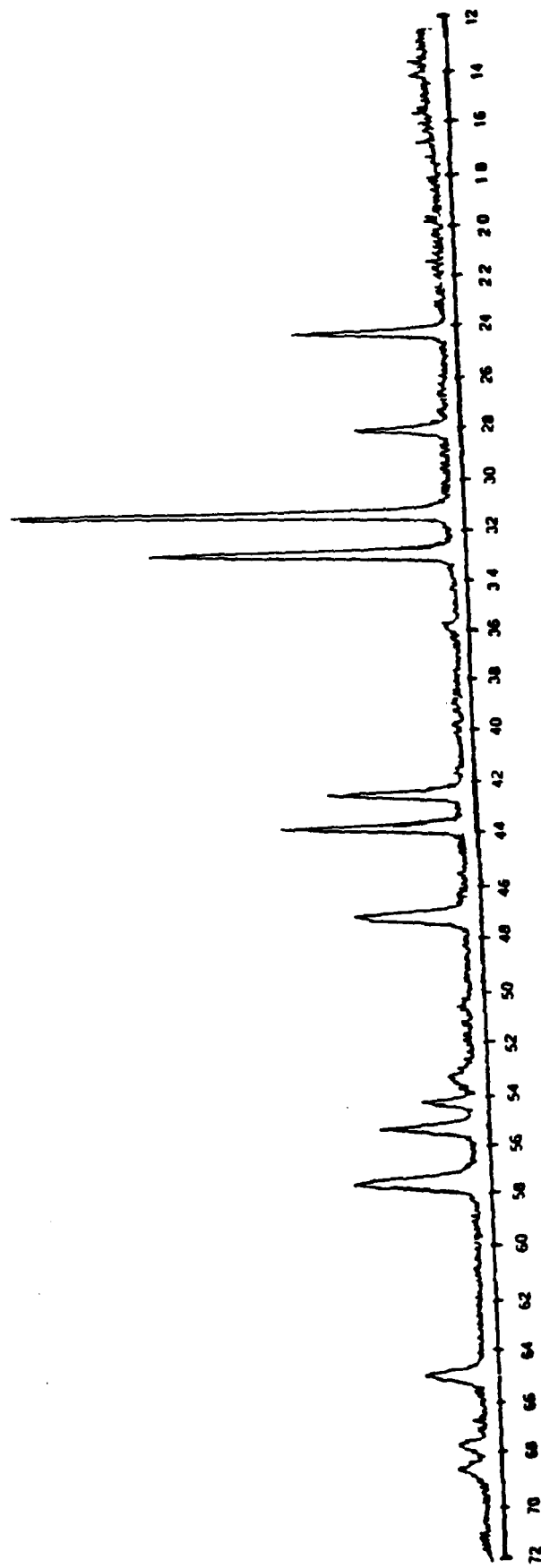


Figure B.10. X-ray diffraction pattern for $\text{La}_{1.1}\text{Ba}_{0.9}\text{NiO}_4$.

Appendix B (cont.)

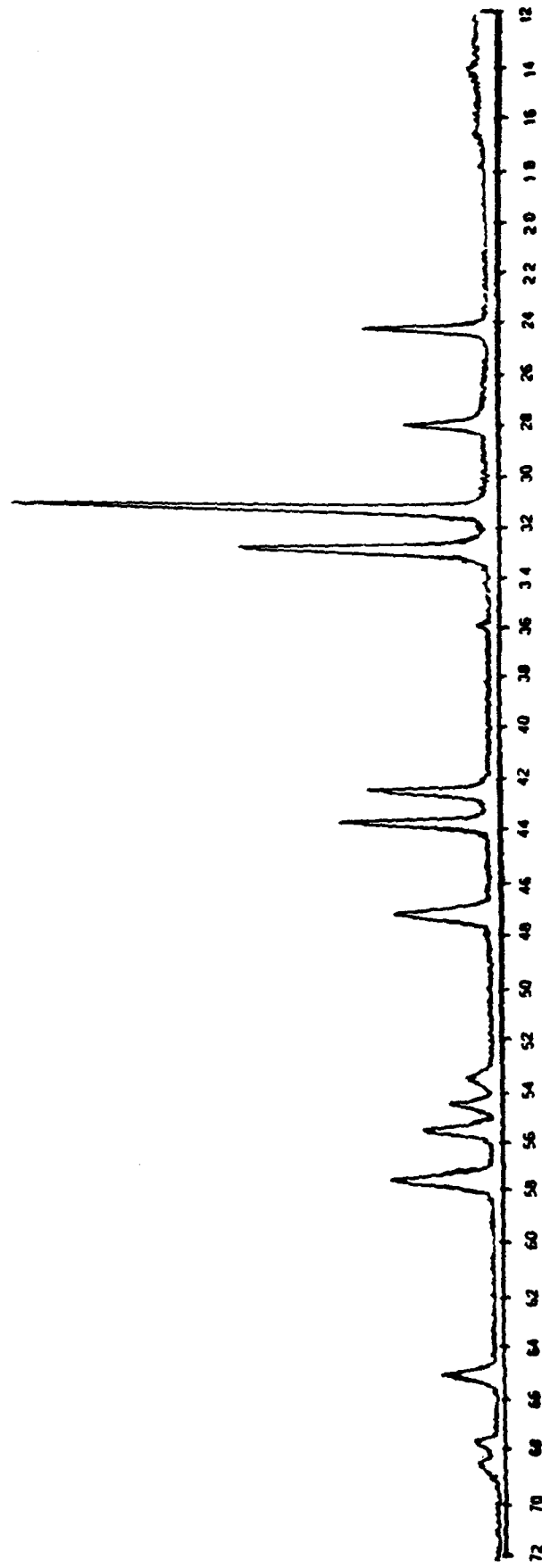


Figure B.11. X-ray diffraction pattern for LaBaNiO₄.

Appendix C

Table C.1 Cell Refinement Data for La_2NiO_4 :

	hkl	THETA OBS	THETA CALC	THETA DIF	d OBS	d CALC
1	002	6.969	6.979	0.01	6.348	6.34
2	101	12.048	12.043	-0.005	3.69	3.692
3	004	14.063	14.063	0	3.17	3.17
4	103	15.688	15.681	-0.006	2.849	2.85
5	110	16.4	16.397	-0.003	2.728	2.729
6	112	17.91	17.898	-0.012	2.505	2.506
7	105	21.322	21.313	-0.009	2.118	2.119
8	006	21.379	21.376	-0.003	2.113	2.113
9	114	21.873	21.868	-0.005	2.068	2.068
10	200	23.533	23.529	-0.004	1.929	1.929
11	211	26.775	26.772	-0.003	1.71	1.71
12	116	27.451	27.453	0.002	1.671	1.671
13	204	27.86	27.862	0.002	1.648	1.648
14	107	28.019	28.019	0	1.64	1.64
15	213	28.824	28.823	-0.001	1.598	1.598
16	008	29.978	29.077	-0.001	1.585	1.585
17	206	32.703	32.723	0.02	1.426	1.425
18	118	34.188	34.196	0.008	1.371	1.37
19	220	34.36	34.372	0.012	1.365	1.365

Appendix C (cont.)

Table C.2 Cell Refinement Data for $\text{La}_{1.9}\text{Ba}_{0.1}\text{NiO}_4$:

	hkl	THETA OBS	THETA CALC	THETA DIF	d OBS	d CALC
1	002	6.95	6.952	0.002	6.366	6.364
2	101	12.043	12.04	-0.003	3.692	3.692
3	004	14.008	14.009	0.001	3.182	3.162
4	103	15.663	15.655	-0.008	2.853	2.854
5	110	16.41	16.399	-0.011	2.726	2.728
6	112	17.898	17.889	-0.009	2.506	2.508
7	105	21.263	21.255	-0.008	2.124	2.125
8	006	21.3	21.292	-0.008	2.12	2.121
9	114	21.835	21.833	-0.002	2.071	2.071
10	200	23.533	23.532	-0.001	1.929	1.929
11	211	26.778	26.774	-0.004	1.71	1.71
12	116	27.382	27.384	0.002	1.675	1.675
13	204	27.833	27.834	0.001	1.65	1.65
14	107	27.923	29.925	0.002	1.645	1.645
15	213	28.8	28.809	0.009	1.599	1.598
16	008	28.95	28.957	0.007	1.591	1.591
17	206	32.667	32.662	-0.005	1.427	1.427
18	118	34.085	34.087	0.002	1.374	1.374
19	220	34.368	34.377	0.009	1.364	1.364

Appendix C (cont.)

Table C.3 Cell Refinement Data for $\text{La}_{1.8}\text{Ba}_{0.2}\text{NiO}_4$

	hkl	THETA OBS	THETA CALC	THETA DIF	d OBS	d CALC
1	002	6.935	6.932	-0.003	6.379	6.382
2	101	12.043	12.046	0.003	3.692	3.691
3	004	13.973	13.968	-0.005	3.190	3.191
4	103	15.640	15.641	0.001	2.857	2.857
5	110	16.410	16.412	0.002	2.726	2.726
6	112	17.885	17.893	0.008	2.508	2.507
7	006	21.225	21.227	-0.002	2.128	2.127
8	114	21.818	21.815	-0.003	2.073	2.073
9	200	23.555	23.551	-0.004	1.927	1.928
10	211	26.795	26.794	-0.001	1.709	1.709
11	116	27.373	27.339	-0.034	1.675	1.677
12	107	27.850	27.858	0.008	1.649	1.648
13	213	28.818	28.817	-0.001	1.598	1.598
14	206	32.630	32.630	0.000	1.428	1.428
15	118	34.015	34.011	-0.004	1.377	1.377
16	220	34.408	34.407	-0.001	1.363	1.363

Appendix C (cont.)

Table C.4 Cell Refinement Data for $\text{La}_{1.7}\text{Ba}_{0.3}\text{NiO}_4$:

	hkl	THETA OBS	THETA CALC	THETA DIF	d OBS	d CALC
1	002	6.9	6.905	0.005	6.411	6.406
2	101	12.068	12.065	-0.003	3.684	3.685
3	004	13.918	13.914	-0.004	3.202	3.203
4	103	15.64	15.631	-0.009	2.857	2.859
5	110	16.46	16.445	-0.015	2.718	2.721
6	112	17.915	17.913	-0.002	2.504	2.504
7	105	21.16	21.17	0.01	2.114	2.133
8	114	21.803	21.804	0.001	2.074	2.074
9	200	23.608	23.601	-0.007	1.923	1.924
10	211	26.85	26.849	-0.001	1.705	1.705
11	116	27.285	27.292	0.007	1.68	1.68
12	107	27.773	27.775	0.002	1.653	1.653
13	204	28.84	27.841	0.001	1.649	1.649
14	008	28.76	28.746	-0.014	1.601	1.602
15	206	32.615	32.607	-0.008	1.429	1.429
16	118	33.91	33.922	0.012	1.381	1.38
17	220	34.477	34.486	0.009	1.361	1.36

Appendix C (cont.)

Table C.5 Cell Refinement Data for $\text{La}_{1.6}\text{Ba}_{0.4}\text{NiO}_4$:

	hkl	THETA OBS	THETA CALC	THETA DIF	d OBS	d CALC
1	002	6.89	6.889	-0.001	6.421	6.421
2	101	12.078	12.07	-0.008	3.681	3.684
3	004	13.878	13.881	0.003	3.211	3.211
4	103	15.63	15.62	-0.01	2.859	2.861
5	110	16.468	16.457	-0.011	2.717	2.719
6	112	17.92	17.917	-0.003	2.503	2.504
7	105	21.12	21.139	0.009	2.137	2.136
8	114	21.79	21.791	0.001	2.075	2.075
9	200	23.62	23.618	-0.002	1.922	1.923
10	211	26.862	26.867	0.005	1.705	1.704
11	116	27.26	27.257	-0.003	1.682	1.682
12	212	27.6	27.626	0.026	1.663	1.661
13	107	27.725	27.721	-0.004	1.656	1.656
14	204	27.825	27.838	0.013	1.65	1.649
15	008	28.713	28.672	-0.041	1.603	1.605
16	213	28.86	28.862	0.002	1.596	1.596
17	206	32.6	32.582	-0.018	1.43	1.43
18	118	33.863	33.861	-0.002	1.382	1.382
19	220	34.575	34.512	-0.063	1.357	1.359

Appendix C (cont.)

Table C.6 Cell Refinement Data for $\text{La}_{1.5}\text{Ba}_{0.5}\text{NiO}_4$:

	hkl	THETA OBS	THETA CALC	THETA DIF	d OBS	d CALC
1	002	6.888	6.88	-0.008	6.423	6.43
2	101	12.093	12.078	-0.015	3.677	3.681
3	004	13.85	13.861	0.011	3.218	3.215
4	103	15.62	15.618	-0.002	2.861	2.861
5	110	16.483	16.471	-0.012	2.715	2.717
6	112	17.938	17.926	-0.012	2.501	2.503
7	105	21.095	21.123	0.028	2.14	2.137
8	114	21.785	21.789	0.004	2.075	2.075
9	200	23.64	23.638	-0.002	1.921	1.921
10	211	26.885	26.89	0.005	1.703	1.703
11	116	27.215	27.241	0.026	1.684	1.683
12	212	27.652	27.647	-0.005	1.66	1.66
13	204	27.825	27.845	0.02	1.65	1.649
14	008	28.59	28.63	0.04	1.61	1.608
15	213	28.865	28.879	0.014	1.6	1.595
16	206	32.585	32.577	-0.008	1.43	1.431
17	118	33.785	33.831	0.046	1.385	1.383
18	220	34.535	34.545	0.01	1.359	1.358

Appendix C (cont.)

Table C.7 Cell Refinement Data for $\text{La}_{1.4}\text{Ba}_{0.6}\text{NiO}_4$

	hkl	THETA OBS	THETA CALC	THETA DIF	d OBS	d CALC
1	002	6.85	6.865	0.015	6.458	6.444
2	101	12.06	12.06	0	3.687	3.687
3	004	13.835	13.832	-0.003	3.221	3.222
4	103	15.59	15.59	0	2.866	2.866
5	110	16.448	16.447	-0.001	2.72	2.72
6	112	17.913	17.899	-0.014	2.504	2.506
7	105	21.073	21.082	0.009	2.142	2.141
8	114	21.75	21.75	0	2.079	2.079
9	200	23.603	23.604	0.001	1.924	1.924
10	211	26.855	26.849	-0.006	1.705	1.705
11	116	27.188	27.187	-0.001	1.686	1.686
12	107	27.62	27.633	0.013	1.661	1.661
13	204	27.775	27.798	0.023	1.6531	1.652
14	213	28.82	28.832	0.012	1.598	1.597
15	206	32.528	32.515	-0.013	1.432	1.433
16	118	33.765	33.757	-0.008	1.386	1.386
17	220	34.49	34.49	0	1.36	1.36

Appendix C (cont.)

Table C.8 Cell Refinement Data for $\text{La}_{1.3}\text{Ba}_{0.7}\text{NiO}_4$:

	hkl	THETA OBS	THETA CALC	THETA DIF	d OBS	d CALC
1	002	6.875	6.871	-0.004	6.435	6.438
2	101	12.05	12.045	-0.005	3.69	3.691
3	004	13.84	13.844	0.004	3.22	3.219
4	103	15.59	15.584	-0.006	2.866	2.867
5	110	16.428	16.424	-0.004	2.724	2.724
6	112	17.875	17.879	0.004	2.509	2.509
7	200	23.575	23.57	-0.005	1.926	1.926
8	211	26.8	26.811	0.011	1.708	1.708
9	116	27.18	27.187	0.007	1.686	1.686
10	107	27.637	27.646	0.009	1.66	1.66
11	204	27.73	27.774	0.044	1.655	1.653
12	008	28.6	28.59	-0.01	1.609	1.61
13	213	28.798	28.799	0.001	1.599	1.599
14	206	32.512	32.501	-0.011	1.433	1.434
15	118	33.763	33.768	0.005	1.386	1.386
16	220	34.438	34.436	-0.002	1.362	1.362

Appendix C (cont.)

Table C.9 Cell Refinement Data for $\text{La}_{1.2}\text{Ba}_{0.8}\text{NiO}_4$:

	hkl	THETA OBS	THETA CALC	THETA DIF	d OBS	d CALC
1	002	6.87	6.881	0.011	6.439	6.429
2	101	12.035	12.032	-0.003	3.694	3.695
3	004	13.873	13.864	-0.009	3.213	3.214
4	103	15.575	15.583	0.008	2.869	2.867
5	110	16.41	16.402	-0.008	2.726	2.728
6	112	17.863	17.863	0	2.511	2.511
7	006	21.075	21.066	-0.009	2.142	2.143
8	114	21.725	21.737	0.012	2.081	2.08
9	200	23.538	23.536	-0.002	1.929	1.929
10	211	26.785	26.773	-0.012	1.709	1.71
11	116	27.17	27.199	0.029	1.687	1.685
12	107	27.685	27.675	-0.01	1.658	1.658
13	008	28.613	28.637	0.024	1.608	1.607
14	213	28.76	28.769	0.009	1.601	1.6
15	206	32.48	32.498	0.018	1.434	1.434
16	118	33.753	33.797	0.044	1.386	1.385
17	220	34.39	34.384	-0.006	1.364	1.364

Appendix C (cont.)

Table C.10 Cell Refinement Data for $\text{La}_{1.1}\text{Ba}_{0.9}\text{NiO}_4$:

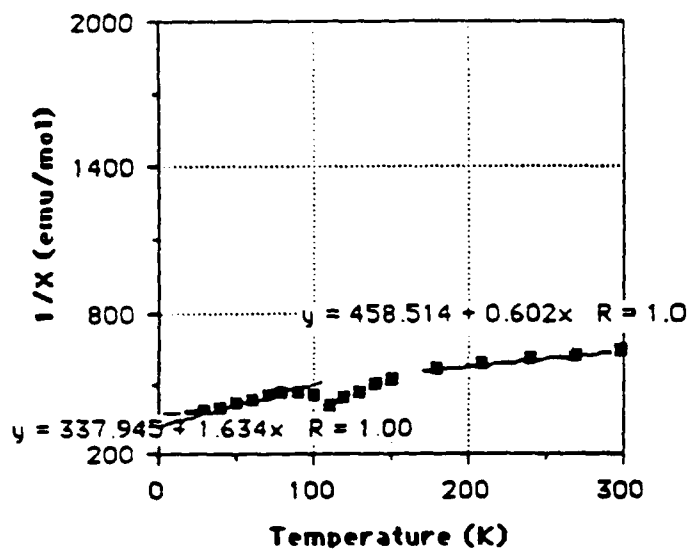
	hkl	THETA OBS	THETA CALC	THETA DIF	d OBS	d CALC
1	002	6.895	6.885	-0.01	6.416	6.425
2	101	12.01	12.011	0.001	3.702	3.701
3	004	13.863	13.873	0.01	3.215	3.213
4	103	15.575	15.57	-0.005	2.869	2.87
5	110	16.37	16.37	0	2.733	2.733
6	112	17.835	17.835	0	2.514	2.515
7	105	21.095	21.095	0	2.14	2.14
8	114	21.71	21.717	0.007	2.082	2.082
9	200	23.493	23.489	-0.004	1.932	1.933
10	211	26.72	26.72	0	1.713	1.713
11	116	27.183	27.188	0.005	1.686	1.686
12	107	27.693	27.678	-0.015	1.657	1.658
13	213	28.723	28.72	-0.003	1.603	1.603
14	206	32.463	32.469	0.006	1.435	1.435
15	118	33.79	33.795	0.005	1.385	1.385
16	220	34.307	34.309	0.002	1.367	1.367

Appendix C (cont.)

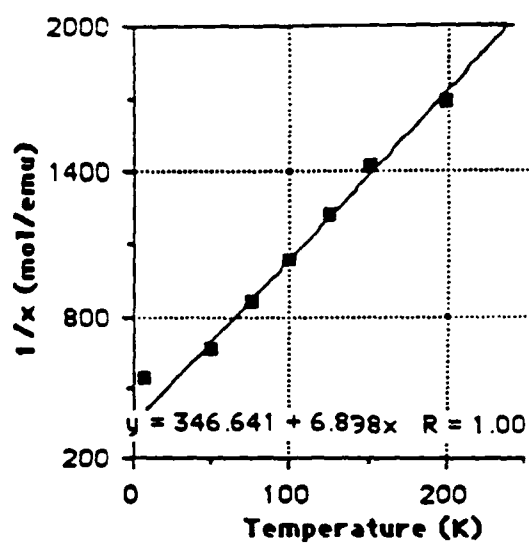
Table C.11 Cell Refinement Data for LaBaNiO₄:

	hkl	THETA OBS	THETA CALC	THETA DIF	d OBS	d CALC
1	002	6.935	6.891	0.044	6.379	6.42
2	101	12	12.003	0.003	3.705	3.704
3	004	13.878	13.885	0.007	3.211	3.21
4	103	15.575	15.569	-0.006	2.869	2.87
5	110	16.35	16.355	0.005	2.736	2.735
6	112	17.838	17.824	-0.014	2.515	2.516
7	105	21.105	21.102	-0.003	2.139	2.139
8	114	21.84	21.714	-0.126	2.07	2.082
9	200	23.463	23.467	0.004	1.935	1.934
10	211	26.813	26.696	-0.117	1.708	1.715
11	116	27.193	27.194	0.001	1.686	1.685
12	204	27.71	27.706	-0.004	1.656	1.657
13	213	28.703	28.701	-0.002	1.604	1.604
14	215	32.475	32.47	-0.005	1.435	1.435
15	118	33.813	33.811	-0.002	1.384	1.384
16	220	34.275	34.276	0.001	1.368	1.368

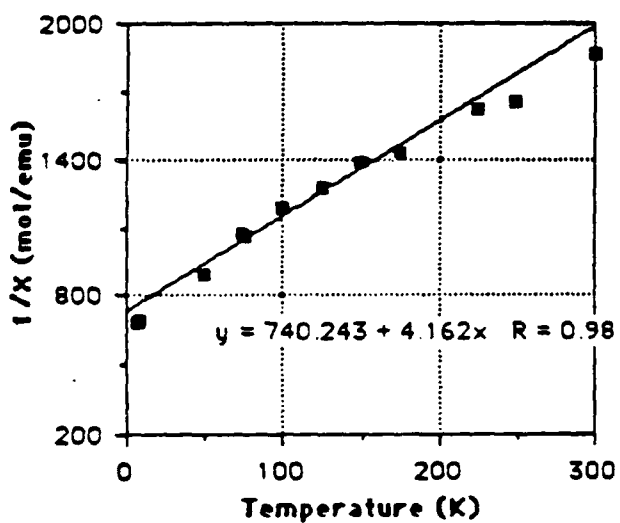
Appendix D



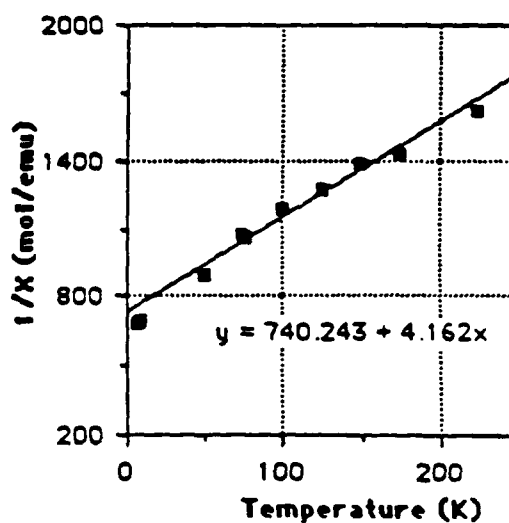
a) La_2NiO_4



b) $\text{La}_{1.8}\text{Ba}_{0.2}\text{NiO}_4$



c) $\text{La}_{1.6}\text{Ba}_{0.4}\text{NiO}_4$



d) $\text{La}_{1.4}\text{Ba}_{0.6}\text{NiO}_4$

Figure D.1 Curie-Weiss law plots for a) La_2NiO_4 in the temperature ranges 6 to 70 K and 180 to 300 K and b) $\text{La}_{1.8}\text{Ba}_{0.2}\text{NiO}_4$, c) $\text{La}_{1.6}\text{Ba}_{0.4}\text{NiO}_4$ and d) $\text{La}_{1.4}\text{Ba}_{0.6}\text{NiO}_4$ in the temperature range 50 to 200 K.

References

1. V. A. Rabenau and P. Eckerlin, *Acta. Crystallogr.* **11**, 304 (1958).
2. R. J. Birgenau, J. Shalo, G. Shirane, *J. Appl. Phys.* **41**, 1303 (1970).
3. G. A. Smolenskii, V. A. Bokov, S. A. Kizaew, E. I. Maltzew, G. M. Nedliev, V. P. Plankty, A. G. Tutov and V. N. Yudin, *Proc. Int. Conf. Magn.*, Nottingham, 354 (1964).
4. P. Ganguly, S. Kollali, C. N. R. Rao and S. Kern *Magn. Lett.* **1**, 107 (1980).
5. C. N. R. Rao, D. J. Buttrey, N. Otsuka, P. Ganguly, H. R. Harrison, C.J. Sandberg and J. M. Honig, *J. Solid State Chem.* **51**, 266 (1984).
6. D. J. Buttrey, J. M. Honig and C. N. R. Rao, *J. Solid State Chem.* **64**, 117 (1986).
7. M. Sayer and P Odier, *J. Solid State Chem.* **67**, 26 (1987).
8. P. Ganguly and C. N. R. Rao, *J. Solid State Chem.* **53**, 193 (1984).
9. Y. Nigara, P. Odier and A. M. Anthony, *Science of Ceramics*, **11** 551 (1981).
10. P. Ganguly and C. N. R. Rao, *Mater. Res. Bull.* **8**, 408 (1973).
11. J. B. Goodenough and S. Ramasesha, *Mater. Res. Bull.* **17**, 383 (1982).
12. J. G. Bednorz and K. A. Müller, *Z. Phys. B.* **64**, 189 (1986).
13. J. Bardeen, L.N. Cooper, and J.R. Schrieffer, *Phys. Rev.* **108**, 1175 (1957).
14. D. Balz and K. Plieth, *Z. Elektrochem.* **59**, 545 (1955).
15. J. F. Ackerman, *Mat. Res. Bull.* **14**, 487 (1979).
16. D. Ganguli, *J. Solid State Chem.* **30**, 353 (1979).
17. P. Poix, *J. Solid State Chem.* **31**, 95 (1980).
18. D. E. Appleman and H. T. Evans, Jr., USGS-GD-73-003, Washington, DC, (1973).
19. Tracor Northern Corp., Middleton, WI.
20. B. L. Morris and A. Wold, *Rev. Sci. Instrum.* **89**, 1937 (1968).
21. J. Gopalakrishnan, G. Colsmann and B. Reuter, *J. Solid State Chem.* **22**, 145 (1977).

22. J. B. Goodenough and P. M. Racciah, *J. Appl. Phys.* **36**, 1031 (1965).
23. R. Ward, *Prog. Inorg. Chem.* **1**, 475 (1959).
24. J. M. Longo and P. M. Racciah, *J. Solid State Chem.* **6**, 526 (1973).
25. D. Babel, *Strct. Bonding* **22**, 145 (1977).
26. G. Blasse, *J. Inorg. Nucl. Chem.* **27**, 2683 (1965).
27. R. D. Shannon and C. T. Prewitt, *Acta. Crystallogr.* **B25**, 925 (1969).
28. H. Obayashi and T. Kudo, *Jap. J. Appl. Phys.* **14**, 330 (1975).
29. D. C. Harris, M. E. Hills and T. A. Hewston, *J. Chem. Ed.* **64**, 847 (1987).
30. D. J. Buttrey, H. R. Harrison, J. M. Honig and R. R. Scharman, *Solid State Chem.* **54**, 407 (1984).
31. J. Drennan, C. P. Tavares and B. C. H. Steele, *Mater. Res. Bull.* **17**, 621 (1982).
32. S. N. Ruddlesden and P. Popper, *Acta. Crystallogr.* **10**, 538 (1957); **11**, 54 (1958).
33. R. A. Mohan Ram, L. Ganapathi, P. Ganguly and C. N. R. Rao, *J. Solid State Chem.* **63**, 139 (1986).
34. K. K. Singh, P. Ganguly and J. B. Goodenough, *J. Solid State Chem.* **52**, 254 (1984).
35. I. Dzialoshininskii, *J. Phys. Chem. Solids* **4**, 241 (1958).
36. T. Moriya, *Phys. Rev.* **120**, 91 (1960).
37. A. S. Shoherbakov, M. I. Katsnel'son, A. V. Trefilov, N. L. Sorokin, E. G. Valiulin and A. N. Petrov., *JETP Letters*, **46**, 136 (1987).
38. M. Crespín, P. Levitz and L. Gatineau, *J. Chem. Soc., Faraday Trans. 2*, **79**, 1181 (1983); **79**, 1195 (1983).
39. L. J. van der Pauw, *Philips Research Reports* **13**, 1 (1958).
40. L. J. van der Pauw, *Phillips Technical Review* **20**, 220 (1958/59).

DISTRIBUTION LIST

No. of Copies	To
1	Office of the Under Secretary of Defense for Research and Engineering, The Pentagon, Washington, DC 20301
	Commander, U.S. Army Laboratory Command, 2800 Powder Mill Road, Adelphi, MD 20783-1145
1	ATTN: AMSLC-IM-TL
	Commander, Defense Technical Information Center, Cameron Station, Building 5, 5010 Duke Street, Alexandria, VA 22304-6145
2	ATTN: DTIC-FDAC
1	Metals and Ceramics Information Center, Battelle Columbus Laboratories, 505 King Avenue, Columbus, OH 43201
	Commander, Army Research Office, P.O. Box 12211, Research Triangle Park, NC 27709-2211
1	ATTN: Information Processing Office
	Commander, U.S. Army Materiel Command, 5001 Eisenhower Avenue, Alexandria, VA 22333
1	ATTN: AMCLD
	Commander, U.S. Army Materiel Systems Analysis Activity, Aberdeen Proving Ground, MD 21005
1	ATTN: AMXSY-MP, H. Cohen
	Commander, U.S. Army Electronics Research and Development Command, Fort Monmouth, NJ 07703
1	ATTN: AMDSD-L
1	AMDSD-E
	Commander, U.S. Army Missile Command, Redstone Scientific Information Center, Redstone Arsenal, AL 35898-5241
1	ATTN: AMSMI-RKP, J. Wright, Bldg. 7574
1	AMSMI-RD-CS-R/Doc
1	AMSMI-RLM
	Commander, U.S. Army Armament, Munitions and Chemical Command, Dover, NJ 07801
2	ATTN: Technical Library
1	AMDAR-LCA, Mr. Harry E. Peibly, Jr., PLASTECH, Director
	Commander, U.S. Army Natick Research, Development, and Engineering Center, Natick, MA 01760
1	ATTN: Technical Library
	Commander, U.S. Army Satellite Communications Agency, Fort Monmouth, NJ 07703
1	ATTN: Technical Document Center
	Commander, U.S. Army Tank-Automotive Command, Warren, MI 4397-5000
1	ATTN: AMSTA-ZSK
2	AMSTA-TSL, Technical Library
	Commander, White Sands Missile Range, NM 88002
1	ATTN: STEWS-WS-VT
	President, Airborne, Electronics and Special Warfare Board, Fort Bragg, NC 28307
1	ATTN: Library
	Director, U.S. Army Ballistic Research Laboratory, Aberdeen Proving Ground, MD 21005
1	ATTN: SLCBR-TSB-S (STINFO)
	Commander, Dugway Proving Ground, Dugway, UT 84022
1	ATTN: Technical Library, Technical Information Division
	Commander, Harry Diamond Laboratories, 2800 Powder Mill Road, Adelphi, MD 20783
1	ATTN: Technical Information Office
	Director, Benet Weapons Laboratory, LCWSL, USA AMCCOM, Watervliet, NY 12189
1	ATTN: AMSMC-LCB-TL
1	AMSMC-LCB-R
1	AMSMC-LCB-RM
1	AMSMC-LCB-RP
	Commander, U.S. Army Foreign Science and Technology Center, 220 7th Street, N.E., Charlottesville, VA 22901
1	ATTN: Military Tech

No. of Copies	To
1	Commander, U.S. Army Aeromedical Research Unit, P.O. Box 577, Fort Rucker, AL 36360 ATTN: Technical Library
1	Director, Eustis Directorate, U.S. Army Air Mobility Research and Development Laboratory, Fort Eustis, VA 23604-5577 ATTN: SAVDL-E-MOS (AVSCOM)
1	U.S. Army Aviation Training Library, Fort Rucker, AL 36360 ATTN: Building 5906-5907
1	Commander, U.S. Army Agency for Aviation Safety, Fort Rucker, AL 36362 ATTN: Technical Library
1	Commander, USACDC Air Defense Agency, Fort Bliss, TX 79916 ATTN: Technical Library
1	Commander, U.S. Army Engineer School, Fort Belvoir, VA 22060 ATTN: Library
1	Commander, U.S. Army Engineer Waterways Experiment Station, P. O. Box 631, Vicksburg, MS 39180 ATTN: Research Center Library
1	Commandant, U.S. Army Quartermaster School, Fort Lee, VA 23801 ATTN: Quartermaster School Library
1	Naval Research Laboratory, Washington, DC 20375 ATTN: Code 5830
2	Dr. G. R. Yoder - Code 6384
1	Chief of Naval Research, Arlington, VA 22217 ATTN: Code 471
1	Edward J. Morrissey, AFWAL/MLTE, Wright-Patterson Air Force, Base, OH 45433
1	Commander, U.S. Air Force Wright Aeronautical Laboratories, Wright-Patterson Air Force Base, OH 45433 ATTN: AFWAL/MLC
1	AFWAL/MLLP, M. Forney, Jr.
1	AFWAL/MLBC, Mr. Stanley Schulman
1	National Aeronautics and Space Administration, Marshall Space Flight Center, Huntsville, AL 35812 ATTN: R. J. Schwinghammer, EH01, Dir, M&P Lab
1	Mr. W. A. Wilson, EH41, Bldg. 4612
1	U.S. Department of Commerce, National Bureau of Standards, Gaithersburg, MD 20899 ATTN: Stephen M. Hsu, Chief, Ceramics Division, Institute for Materials Science and Engineering
1	Committee on Marine Structures, Marine Board, National Research Council, 2101 Constitution Ave., N.W., Washington, DC 20418
1	Librarian, Materials Sciences Corporation, Guynedd Plaza 11, Bethlehem Pike, Spring House, PA 19477
1	The Charles Stark Draper Laboratory, 68 Albany Street, Cambridge, MA 02139
1	Wyman-Gordon Company, Worcester, MA 01601 ATTN: Technical Library
1	Lockheed-Georgia Company, 86 South Cobb Drive, Marietta, GA 30063 ATTN: Materials and Processes Engineering Dept. 71-11, Zone 54
1	General Dynamics, Convair Aerospace Division, P.O. Box 748, Fort Worth, TX 76101 ATTN: Mfg. Engineering Technical Library
1	Mechanical Properties Data Center, Belfour Stulen Inc., 13917 W. Bay Shore Drive, Traverse City, MI 49684
1	Mr. R. J. Zentner, EAI Corporation, 626 Towne Center Drive, Suite 205, Joppatowne, MD 21085-4440
2	Director, U.S. Army Materials Technology Laboratory, Watertown, MA 02172-0001 ATTN: SLCMT-TML
1	Author

U.S. Army Materials Technology Laboratory,
Watertown, Massachusetts 02172-0001
CRYSTAL CHEMISTRY, MAGNETIC AND ELECTRICAL
PROPERTIES OF $\text{La}_{2-x}\text{Ba}_x\text{NiO}_4$ - Amy B. Austin

Technical Report MTL TR 89-10, February 1989, 78 pp -
illus-tables, D/A Project IL161102AH42

AD

UNCLASSIFIED
UNLIMITED DISTRIBUTION
 K_2NiF_4 structure
Jahn-Teller effect
Oxygen stoichiometry

The series of compositions $\text{La}_{2-x}\text{Ba}_x\text{NiO}_4$ ($0 \leq x \leq 1.0$) was prepared by standard ceramic techniques. All of the members of the system crystallized with the tetragonal K_2NiF_4 structure. The ratio of lattice parameters, c/a , reached a maximum in the range $x = 0.5$ to 0.6 ; c increased up to this point while a decreased, and this trend reversed after the maximum was reached. The increase in c/a is attributed to a weak Jahn-Teller distortion due to octahedral site low-spin Ni^{3+} ions. Magnetic susceptibilities measured in the temperature range 6 to 300 K and room temperature resistivity measurements showed that with the addition of any barium into the system, a significant change was seen in both the magnetic and electrical properties. An anomaly in the magnetic susceptibility was seen at 110 K in La_2NiO_4 . This anomaly disappeared and the magnetic susceptibility dropped by a factor of at least one-third with the addition of barium into the system. With further increases in barium, the susceptibility value did not differ significantly in all Ba-substituted compounds. The room temperature resistivity dropped from 0.14 $\Omega\text{-cm}$ for La_2NiO_4 to 0.05 $\Omega\text{-cm}$ for $\text{La}_1.88\text{Ba}_0.2\text{NiO}_4$ and decreased only slightly thereafter with increasing amounts of barium. Semiconducting behavior was observed for all of the compounds. Oxygen stoichiometry is suspected to play a critical role in the explanation of these behaviors.

U.S. Army Materials Technology Laboratory,
Watertown, Massachusetts 02172-0001
CRYSTAL CHEMISTRY, MAGNETIC AND ELECTRICAL
PROPERTIES OF $\text{La}_{2-x}\text{Ba}_x\text{NiO}_4$ - Amy B. Austin

Technical Report MTL TR 89-10, February 1989, 78 pp -
illus-tables, D/A Project IL161102AH42

AD

UNCLASSIFIED
UNLIMITED DISTRIBUTION
 K_2NiF_4 structure
Jahn-Teller effect
Oxygen stoichiometry

The series of compositions $\text{La}_{2-x}\text{Ba}_x\text{NiO}_4$ ($0 \leq x \leq 1.0$) was prepared by standard ceramic techniques. All of the members of the system crystallized with the tetragonal K_2NiF_4 structure. The ratio of lattice parameters, c/a , reached a maximum in the range $x = 0.5$ to 0.6 ; c increased up to this point while a decreased, and this trend reversed after the maximum was reached. The increase in c/a is attributed to a weak Jahn-Teller distortion due to octahedral site low-spin Ni^{3+} ions. Magnetic susceptibilities measured in the temperature range 6 to 300 K and room temperature resistivity measurements showed that with the addition of any barium into the system, a significant change was seen in both the magnetic and electrical properties. An anomaly in the magnetic susceptibility was seen at 110 K in La_2NiO_4 . This anomaly disappeared and the magnetic susceptibility dropped by a factor of at least one-third with the addition of barium into the system. With further increases in barium, the susceptibility value did not differ significantly in all Ba-substituted compounds. The room temperature resistivity dropped from 0.14 $\Omega\text{-cm}$ for La_2NiO_4 to 0.05 $\Omega\text{-cm}$ for $\text{La}_1.88\text{Ba}_0.2\text{NiO}_4$ and decreased only slightly thereafter with increasing amounts of barium. Semiconducting behavior was observed for all of the compounds. Oxygen stoichiometry is suspected to play a critical role in the explanation of these behaviors.

U.S. Army Materials Technology Laboratory,
Watertown, Massachusetts 02172-0001
CRYSTAL CHEMISTRY, MAGNETIC AND ELECTRICAL
PROPERTIES OF $\text{La}_{2-x}\text{Ba}_x\text{NiO}_4$ - Amy B. Austin

Technical Report MTL TR 89-10, February 1989, 78 pp -
illus-tables, D/A Project IL161102AH42

AD

UNCLASSIFIED
UNLIMITED DISTRIBUTION
 K_2NiF_4 structure
Jahn-Teller effect
Oxygen stoichiometry

The series of compositions $\text{La}_{2-x}\text{Ba}_x\text{NiO}_4$ ($0 \leq x \leq 1.0$) was prepared by standard ceramic techniques. All of the members of the system crystallized with the tetragonal K_2NiF_4 structure. The ratio of lattice parameters, c/a , reached a maximum in the range $x = 0.5$ to 0.6 ; c increased up to this point while a decreased, and this trend reversed after the maximum was reached. The increase in c/a is attributed to a weak Jahn-Teller distortion due to octahedral site low-spin Ni^{3+} ions. Magnetic susceptibilities measured in the temperature range 6 to 300 K and room temperature resistivity measurements showed that with the addition of any barium into the system, a significant change was seen in both the magnetic and electrical properties. An anomaly in the magnetic susceptibility was seen at 110 K in La_2NiO_4 . This anomaly disappeared and the magnetic susceptibility dropped by a factor of at least one-third with the addition of barium into the system. With further increases in barium, the susceptibility value did not differ significantly in all Ba-substituted compounds. The room temperature resistivity dropped from 0.14 $\Omega\text{-cm}$ for La_2NiO_4 to 0.05 $\Omega\text{-cm}$ for $\text{La}_1.88\text{Ba}_0.2\text{NiO}_4$ and decreased only slightly thereafter with increasing amounts of barium. Semiconducting behavior was observed for all of the compounds. Oxygen stoichiometry is suspected to play a critical role in the explanation of these behaviors.

U.S. Army Materials Technology Laboratory,
Watertown, Massachusetts 02172-0001
CRYSTAL CHEMISTRY, MAGNETIC AND ELECTRICAL
PROPERTIES OF $\text{La}_{2-x}\text{Ba}_x\text{NiO}_4$ - Amy B. Austin

Technical Report MTL TR 89-10, February 1989, 78 pp -
illus-tables, D/A Project IL161102AH42

AD

UNCLASSIFIED
UNLIMITED DISTRIBUTION
 K_2NiF_4 structure
Jahn-Teller effect
Oxygen stoichiometry

The series of compositions $\text{La}_{2-x}\text{Ba}_x\text{NiO}_4$ ($0 \leq x \leq 1.0$) was prepared by standard ceramic techniques. All of the members of the system crystallized with the tetragonal K_2NiF_4 structure. The ratio of lattice parameters, c/a , reached a maximum in the range $x = 0.5$ to 0.6 ; c increased up to this point while a decreased, and this trend reversed after the maximum was reached. The increase in c/a is attributed to a weak Jahn-Teller distortion due to octahedral site low-spin Ni^{3+} ions. Magnetic susceptibilities measured in the temperature range 6 to 300 K and room temperature resistivity measurements showed that with the addition of any barium into the system, a significant change was seen in both the magnetic and electrical properties. An anomaly in the magnetic susceptibility was seen at 110 K in La_2NiO_4 . This anomaly disappeared and the magnetic susceptibility dropped by a factor of at least one-third with the addition of barium into the system. With further increases in barium, the susceptibility value did not differ significantly in all Ba-substituted compounds. The room temperature resistivity dropped from 0.14 $\Omega\text{-cm}$ for La_2NiO_4 to 0.05 $\Omega\text{-cm}$ for $\text{La}_1.88\text{Ba}_0.2\text{NiO}_4$ and decreased only slightly thereafter with increasing amounts of barium. Semiconducting behavior was observed for all of the compounds. Oxygen stoichiometry is suspected to play a critical role in the explanation of these behaviors.